




N6-methyladenosine RNA modification regulates cotton drought response in a Ca²⁺ and ABA-dependent manner

Baoqi Li^{1,†}, Mengmeng Zhang^{1,†}, Weinan Sun¹, Dandan Yue¹, Yizan Ma¹, Boyang Zhang¹, Lingfeng Duan², Maojun Wang¹ , Keith Lindsey³, Xinhui Nie^{4,*}, Xianlong Zhang¹  and Xiyan Yang^{1,*} 

¹National Key Laboratory of Crop Genetic Improvement, Huazhong Agricultural University, Wuhan, Hubei, China

²College of Engineering, Huazhong Agricultural University, Wuhan, Hubei, China

³Department of Biosciences, Durham University, Durham, UK

⁴Key Laboratory of Oasis Ecology Agricultural of Xinjiang Bingtuan, Agricultural College, Shihezi University, Xinjiang, China

Received 9 August 2022;

revised 10 February 2023;

accepted 24 February 2023.

*Correspondence (Xiyan Yang: Tel +86-27-87283955; Fax: +86-27-87280196; email xyx@mail.hzau.edu.cn; Xinhui Nie: Tel +86 18139283069; Fax: +86-99-32058970; email xjnxh2004130@126.com)

[†]These authors contributed equally to this work.

Summary

N⁶-methyladenosine (m⁶A) is the most prevalent internal modification present in mRNAs, and is considered to participate in a range of developmental and biological processes. Drought response is highly regulated at the genomic, transcriptional and post-transcriptional levels. However, the biological function and regulatory mechanism of m⁶A modification in the drought stress response is still poorly understood. We generated a transcriptome-wide m⁶A map using drought-resistant and drought-sensitive varieties of cotton under different water deficient conditions to uncover patterns of m⁶A methylation in cotton response to drought stress. The results reveal that m⁶A represents a common modification and exhibit dramatic changes in distribution during drought stress. More 5'UTR m⁶A was deposited in the drought-resistant variety and was associated with a positive effect on drought resistance by regulating mRNA abundance. Interestingly, we observed that increased m⁶A abundance was associated with increased mRNA abundance under drought, contributing to drought resistance, and vice versa. The demethylase GhALKBH10B was found to decrease m⁶A levels, facilitating the mRNA decay of ABA signal-related genes (*GhZEP*, *GhNCED4* and *GhPP2CA*) and Ca²⁺ signal-related genes (*GhECA1*, *GhCNGC4*, *GhANN1* and *GhCML13*), and mutation of *GhALKBH10B* enhanced drought resistance at seedling stage in cotton. Virus-induced gene silencing (VIGS) of two Ca²⁺-related genes, *GhECA1* and *GhCNGC4*, reduced drought resistance with the decreased m⁶A enrichment on silenced genes in cotton. Collectively, we reveal a novel mechanism of post-transcriptional modification involved in affecting drought response in cotton, by mediating m⁶A methylation on targeted transcripts in the ABA and Ca²⁺ signalling transduction pathways.

Keywords: Cotton, Ca²⁺ signalling pathway, Drought stress, GhALKBH10B, mRNA stability, N⁶-methyladenosine.

Introduction

N⁶-methyladenine (m⁶A) is a methylation modification occurring at the 6th N atom of adenine in RNA, and is widely distributed, in mammals, plants, fruit flies, yeasts, and viruses (Cantara *et al.*, 2011; Wei *et al.*, 2017). The levels of m⁶A mRNA methylation are promoted by methyltransferase complexes, named as “writers” (Liu *et al.*, 2014b; Ping *et al.*, 2014; Wang *et al.*, 2016b), and removed by m⁶A demethylases, named as “erasers” (Jia *et al.*, 2011; Zheng *et al.*, 2013). The m⁶A-modified transcripts are recognized by the “reader” proteins, which mediate the downstream effects of the m⁶A modification (Wang *et al.*, 2015; Xu *et al.*, 2014). In mammals, METTL3/METTL14 act as core methyltransferase to form a complex with other subunits (such as WTAP and VIRMA, etc.), which synergizes with m⁶A methylation modification in mature mRNA (Liu *et al.*, 2014b; Ping *et al.*, 2014; Yue *et al.*, 2018). FTO and ALKBH5 are responsible for removing m⁶A modifications on adenine (Zheng *et al.*, 2013). Plant m⁶A methyltransferase complex components such as MTA, MTB, FIP37 (homologous to mammalian METTL3, METTL14, and WTAP), VIR, HAKAI (Ping *et al.*, 2014; Růžicka *et al.*, 2017; Zhong *et al.*, 2008), demethylase ALKBH9B and ALKBH10B (Martinez-Perez *et al.*, 2017; Zheng *et al.*, 2013), and reading proteins such

as ECT2, ECT3, ECT4 and CPSF30-L (homologous to the YTH family in mammals) (Arribas-Hernandez *et al.*, 2018; Scutenaire *et al.*, 2018; Song *et al.*, 2021; Wei *et al.*, 2018) have also been identified and characterized. Through the interaction between methyltransferases and demethylases, m⁶A is dynamically balanced in organisms, resulting in docking sites for m⁶A binding proteins and appropriate assembly of RNA secondary structures (Liu *et al.*, 2015).

Most studies have shown that m⁶A is enriched near the 3'UTR in mammals and plants, and reading proteins participate in the regulation of mRNA stability or translation process by targeting this region (Luo *et al.*, 2020; Miao *et al.*, 2022; Zhou *et al.*, 2022). Moreover, the m⁶A methylation occurs in conserved sequence context as RRACH and plant-specific motif URUAY, with some specific sequence preferences in different plants or different tissues (Duan *et al.*, 2017; Luo *et al.*, 2020; Wei *et al.*, 2018; Zhou *et al.*, 2022). As a dynamic and reversible post-transcriptional modification, the m⁶A modification affects almost all aspects of RNA processing, including RNA splicing, RNA stability, nuclear retention, and translation efficiency (Anderson *et al.*, 2018; Dominissini *et al.*, 2012; Fu *et al.*, 2014; Liang *et al.*, 2020; Meyer *et al.*, 2012; Wang *et al.*, 2014; Zhao *et al.*, 2014, 2017; Zhou *et al.*, 2015), thus participating in different developmental and

biological processes, including cell fate determination, trichome branching, flowering transition, stress responses, spore development, and fruit maturation in plants (Arribas-Hernandez *et al.*, 2018; Hu *et al.*, 2021; Scutenaire *et al.*, 2018; Song *et al.*, 2021; Zhang *et al.*, 2019; Zhou *et al.*, 2019, 2021).

Drought is one of the most important environmental factors affecting crop distribution, plant development and yield production worldwide. During the long evolutionary process, plants have developed many response mechanisms to drought stress at physiological, biochemical, cellular and molecular levels, including the regulation of osmotic regulatory substances, reactive oxygen defence systems, stomatal conductance, as well as the activation of signal transduction pathways, such as Ca^{2+} signalling and ABA signalling pathways, transcription factor activation and genes responsible for controlling ion homeostasis (Dittrich *et al.*, 2019; Gupta *et al.*, 2020; Rodrigues *et al.*, 2019; Saxena *et al.*, 2016; Su *et al.*, 2013; Tardieu *et al.*, 2018). Consequently, m⁶A-mediated abiotic stress responses were studied in maize (Miao *et al.*, 2020), wheat (Sun *et al.*, 2020), pak-choi (Liu *et al.*, 2020), sweet sorghum (Zheng *et al.*, 2021), rice (Cheng *et al.*, 2021), tomato (Yang *et al.*, 2021), sea buckthorn (Zhang *et al.*, 2021), cotton (Wang *et al.*, 2022), apple (Hou *et al.*, 2022) and barley (Su *et al.*, 2022). These results reveal that m⁶A modification participates in controlling the responses of crops to abiotic stress, including drought stress. However, the characteristics and regulatory mechanisms of m⁶A in cotton response to drought stress have not been defined. Cotton (*Gossypium hirsutum* L.) is an important worldwide commercial crop grown as a source of natural fibre and edible oil. In a previous study, we characterized two upland cotton varieties which were identified as drought-sensitive accession ZY7 and drought-resistant accession ZY168, using an automatic phenotyping platform to acquire several i-traits used as indicators for drought response in cotton (Li *et al.*, 2020). Here, we describe transcriptome-wide m⁶A methylation identification, and investigate the dynamic regulation of m⁶A in cotton under different water deficient conditions using these two varieties, and determine its biological significance by disturbing the expression of the m⁶A eraser ALKBH10. The results reveal that m⁶A represents a prevalent modification and exhibit dramatically dynamic distribution during drought stress. We show that decreased m⁶A modification by the demethylase GhALKBH10B reduces mRNA stability of genes in the Ca^{2+} and ABA signalling pathways, thereby facilitating the drought response of cotton. Moreover, virus-induced gene silencing (VIGS)-mediated knock-down of genes related to the Ca^{2+} signalling pathway reduced drought tolerance through effects on ion exchange. Our study uncovers the regulatory effects of m⁶A methylation on drought response and reveals a direct role for m⁶A methylation in the regulation of key elements in the Ca^{2+} signalling pathway.

Results

m⁶A distribution exhibits a dramatic change during drought stress in cotton

To investigate whether m⁶A methylation participates in modulating cotton drought response, liquid chromatography tandem mass spectrometry (LC–MS/MS) was used to characterize the m⁶A levels during dynamic drought stress using two upland cotton varieties (*Gossypium hirsutum*), which were identified as drought-sensitive (accession ZY7) and drought-resistant (accession ZY168). The drought treatments were conducted as in our previous study (Li *et al.*, 2020) (Figure 1a). RNA was isolated from leaf of the two

varieties at three time points i.e. mild drought (MD), severe drought (SD), and re-watering after drought (RD). These samples were named as MT (samples from mild drought treatment), ST (samples from severe drought treatment) and RT (samples from re-watering after drought) and their parallel controls (MC, SC and RC) were used to conduct the experiments. LC–MS/MS analysis revealed a dramatic change of m⁶A distribution under different water deficient conditions, whereby the methylation levels of N⁶-methyladenine (m⁶A/A) in mRNA of the two cotton varieties at the seedling stage ranged from 0.36% to 0.59% (Figure 1b). The overall m⁶A/A showed no significant difference between treatment and control under MD, but significant increasing was observed under SD in both cotton varieties, with the ratio of m⁶A/A increasing from 0.44% to 0.57% in ZY7 and from 0.51% to 0.59% in ZY168. Meanwhile, the ratios of m⁶A/A were higher in drought-resistant ZY168 than drought-sensitive ZY7 at MD under treatments and controls. However, the value of m⁶A/A decreased in droughted plants and showed no significant difference compared with the control after relieving drought stress. The results show that drought stress basically promotes the m⁶A content in cotton, however with significant differences in drought-sensitive and drought-resistant varieties.

m⁶A features in cotton under different drought conditions

m⁶A-immunoprecipitation (IP) and matched input (non-IP control) libraries of ZY7 and ZY168 were constructed and sequenced under MD, SD and RD conditions and subjected to massively parallel sequencing (Dominissini *et al.*, 2013). The average data size of valid bases in MeRIP-seq was 9.59G and 6.05G for input and IP samples, and the mean transcript coverage of input and IP was 41.25X and 26.08X in clean data (Table S1). The correlation analyses showed a good duplication between biological replicates that R^2 ranged from 0.947 to 0.994 in input samples, and 0.965 to 0.990 in IP samples (Figures S1 and S2). These results suggest the dynamic change of mRNA transcription under different drought treatments as well as good consistency between the biological replicates.

Peak numbers from MeRIP data reached saturation point when the input and m⁶A-IP of mRNA reads reached a plateau of 40 million for each sample (Figure S3). The high-confident consistent peaks (identified in both biological replicates) were used for the following analysis (Table S2). The results of peak calling showed that total number of consistent m⁶A peak could be identified ranging from 20 755 to 25 731 between the two cotton varieties under different watering regimes. The m⁶A profile of all peaks identified in two varieties under different drought condition in treatment with its parallel control panel was shown in Figure 1c. Comparing the conservative m⁶A peaks in the two cotton varieties, it was found that the number of peaks decreased with severe water stress (Figure S4).

The differentially methylated peaks (with differentially m⁶A methylated enrichment under Treatment/Control, FDR < 0.05) and the related differentially methylated transcripts (DMeTs) were obtained for further analysis (Table S2). 1266 and 1202 differentially methylated peaks were presented in ZY7 under MD and SD respectively, and 1841 and 1294 differentially methylated peaks under MD and SD respectively in ZY168 (Figure 2a). After RD, the DMeTs decreased to 732 and 526 in ZY7 and ZY168, respectively. Meanwhile, a total of 4420 non-redundant DMeTs with average peaks (ratio of peak and transcript number) ranged from 1.04 to 1.12 across different

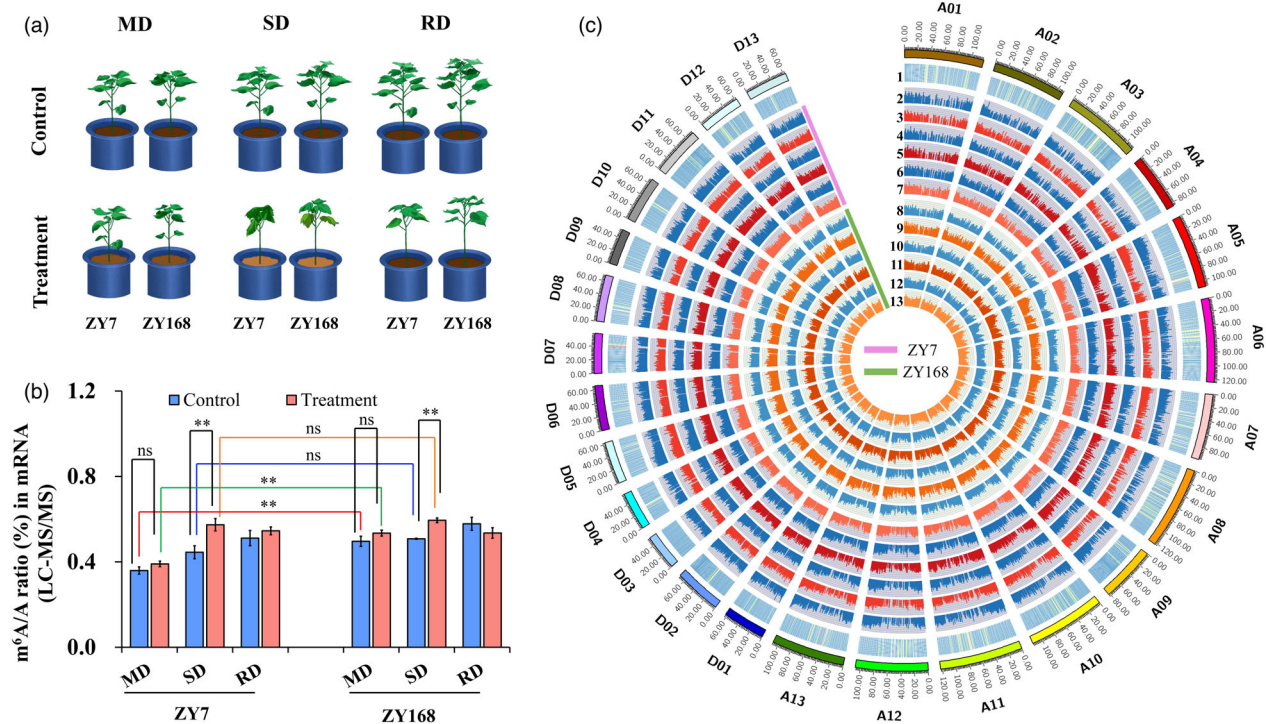


Figure 1 Transcriptome-wide m⁶A methylome profiling in cotton. (a) Diagrammatic representation of the drought-sensitive accession ZY7 and drought-resistant accession ZY168 under mild drought (MD), severe drought (SD), and re-watering after drought (RD) conditions. (b) m⁶A percentage relative to adenosine (m⁶A/A ratio) determined by LC–MS/MS in mRNA of ZY7 and ZY168 under different treatments. Error bars represent standard deviations (SD) based on three biological replicates, statistical significance was determined by a two-sided *t*-test: ** *P* < 0.01. ns, no significance. (c) Circos plot showing the m⁶A peak distribution at the whole transcriptome scale of both ZY7 and ZY168. The outermost track represents the 26 chromosomes (A01–A13, D01–D13) of *Gossypium hirsutum* genome. Track 1 represents the adenosine density, and data were analysed with a bin size of 1-Mb. The other tracks (track 2–13) represent the log₂ fold enrichment of m⁶A peak with value (0–10) on y-axis from different samples: 2–7, represent all consistent m⁶A peaks identified in ZY7 from samples of MC, MT, SC, ST, RC and RT respectively; 8–13, represent all consistent m⁶A peaks identified in ZY168 from samples MC, MT, SC, ST, RC and RT respectively. MT, ST and RT mean samples from MD, SD and RD conditions and their parallel controls (MC, SC and RC).

conditions in these two cotton varieties (Figure 2a). Next, HOMER was applied to analyse the motif enrichment sequence within m⁶A peaks in cotton. Notably, the widely-conserved motif RRACH (R = A/G; H = A/C/U) and plant-specific motif UGUA found in *Arabidopsis* (Wei *et al.*, 2018), tomato (Zhou *et al.*, 2019), maize (Luo *et al.*, 2020) and apple (Hou *et al.*, 2022) was identified in cotton (Figure 2b). Moreover, we also newly identified DGCAG (D = A/G/U) and 5' deposited motif CAAUG motif in cotton (Figure 2b; Table S3).

We then evaluated the distribution of m⁶A peaks in the whole transcriptome of cotton during dynamic drought treatments. m⁶A peaks were largely enriched in 3'UTRs, which is consistent with previous reports in other plants and mammals (Zhou *et al.*, 2022). For drought-sensitive variety ZY7, the proportion of m⁶A peaks located in different regions showed little changes (<1%) in the percentage ratio in treatments compared with controls from MD to RD. Surprisingly, an obvious apiciform was found in drought-resistant variety ZY168 under both MD and SD with m⁶A peaks enriched near the 5'UTR (in the 5'UTR or the 1st exon) in drought treatments compared with the corresponding controls, with the proportions increased from 6.4% to 8.8% under MD, and from 6.4% to 9.5% under SD. However, the differences in the proportions were not obvious between the droughted and control plants under RD. We also identified more

5'UTR deposited m⁶A peaks and m⁶A modified transcripts in drought-resistant variety ZY168 (762 peaks on 594 transcripts) than in drought-sensitive variety ZY7 (310 peaks on 288 transcripts) (Figure 2c, d; Tables S4 and S5). These data not only suggest that drought has a critical influence in m⁶A peak distribution, but also demonstrates the dynamics and complexity of m⁶A modification in cotton.

m⁶A methylation affects the abundance of significant DMeTs under drought stress conditions in cotton

To explore whether m⁶A methylation influences the abundance of DMeTs under drought conditions, the significant differentially m⁶A methylated peaks (FDR < 0.05, m⁶A foldchange > 1.5) within DMeTs were used for further analysis (Tables S4 and S5), following the reported criterion (Zhou *et al.*, 2021). As a result, the changes of significant DMeTs abundance displayed a positive correlation with the fold change of m⁶A enrichment for the drought-sensitive variety (ZY7) under MD and both varieties under SD, but not under RD, which suggested m⁶A methylation might affect the abundance of significant DMeTs under drought stress conditions (Figure S5). As shown in Figure 3a, 667, 680 and 202 downregulated m⁶A peaks and 292, 151 and 249 upregulated peaks were identified under MD, SD and RD in ZY7 (Table S4). Significant differences could be seen when

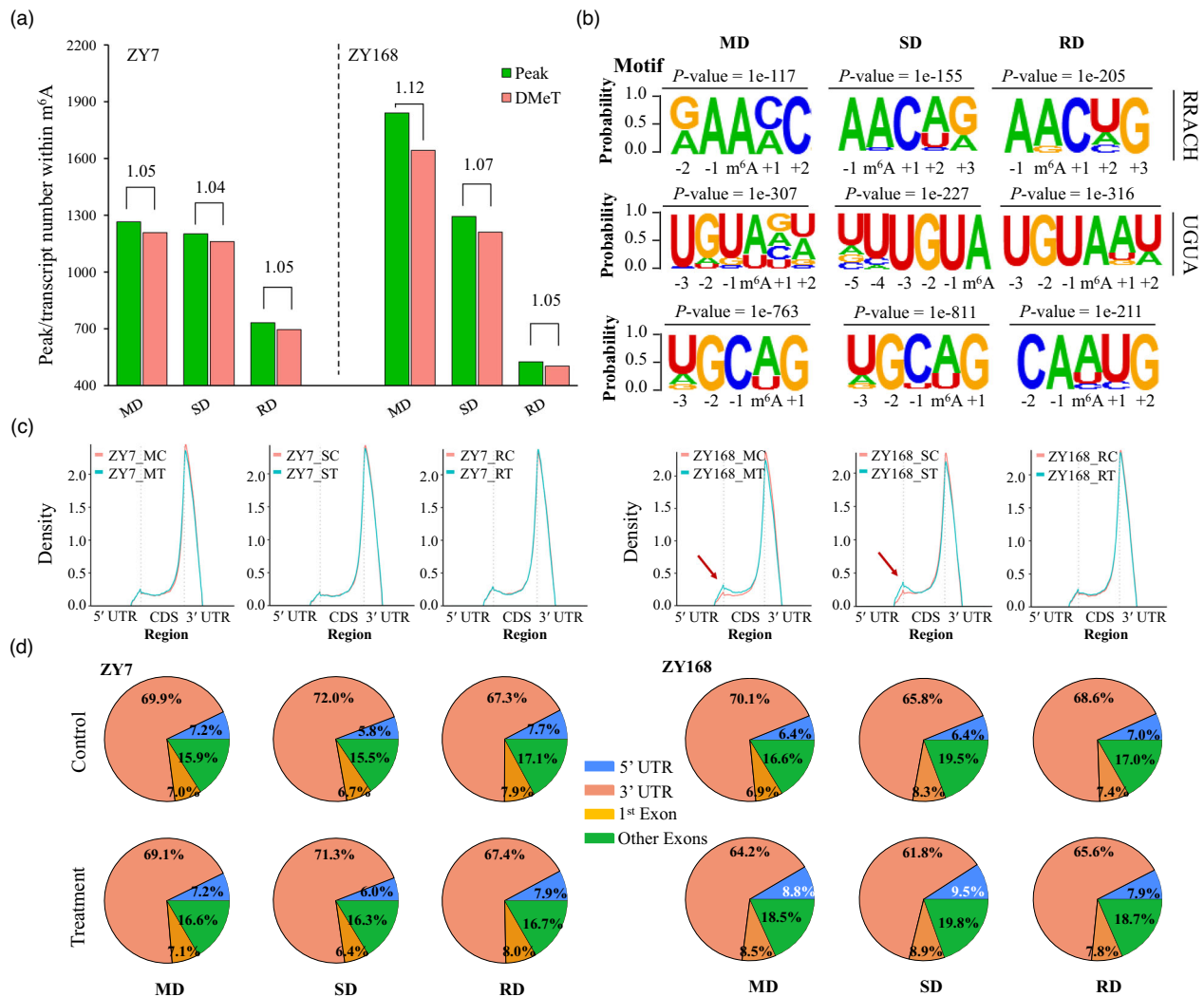


Figure 2 Dynamic distribution of m⁶A under different drought conditions. (a) The number of differentially methylated m⁶A peak (treatment/control) and differentially methylated transcripts (DMeTs) under mild drought (MD), severe drought (SD), and re-watering after drought (RD) conditions. Value of average differentially methylated m⁶A peaks in each DMeT (ratio of peak and transcript number) is shown above the column under different drought conditions. (b) Enriched m⁶A motifs in cotton under drought treatments. RRACH and UGUA were conserved motif among plants, DGCAG and CAAUG were newly identified motif in cotton. R represents A/G, H represents A/C/U, D represents A/G/U. (c) Density of m⁶A deposited site on the regions within transcripts. Arrows in red represent a tag indicating the sharply increased m⁶A peak deposited in the 5' UTR in ZY168 under MD and SD. (d) Called peaks were annotated with four regions of transcripts (5'UTR, 1st exon, other exon and 3'UTR) under MD, SD, and RD.

comparing downregulated and upregulated group under MD ($P = 1.02 \times 10^{-9}$), SD ($P = 1.13 \times 10^{-5}$), and RD ($P = 7.04 \times 10^{-5}$). We did the same analysis in ZY168, and 228, 334 and 35 downregulated m⁶A peaks were identified under MD, SD and RD, with 957, 669 and 267 upregulated peaks (Table S5). Highly significant differences ($P < 0.01$) were only found between downregulated and upregulated group under SD ($P = 2.2 \times 10^{-16}$), but not under MD ($P = 0.02$) and RD ($P = 0.11$).

We analysed the relationship between significant DMeTs abundance and m⁶A enrichment regions of the transcripts (Tables S4 and S5). The percentage of peaks enriched in the 5'UTR increased to 33.8% and 27.5% under MD and SD in ZY168, compared to 10.3% and 11.3% in ZY7. Significant differences ($P < 0.05$) were found between significant DMeTs levels of the group with m⁶A enrichment at the 3'UTR and 5'UTR

regions under droughted conditions. While, the m⁶A-deposited regions also affected the mRNA abundance of DMeTs, for that the significant DMeTs with exon-deposited m⁶A methylation exhibited relatively lower down-regulation than 5'UTR-deposited m⁶A methylation in ZY168 under MD and in ZY7 under SD, and no significance between different regions under RD - this was also seen in the cumulative curve results (Figure 3b; Figure S6). Interestingly, under SD, peaks enriched at the 5'UTR (27.5%) exhibited higher mRNA abundance of significant DMeTs compared to 3'UTR in ZY168, but lower abundance compared to 3'UTR enrichment in ZY7. We would propose that there is differential m⁶A deposition at the 5'UTR in drought-resistance ZY168 and drought-sensitive ZY7 under drought conditions, with a positive effect on drought resistance through the effects on abundance of significant DMeTs.

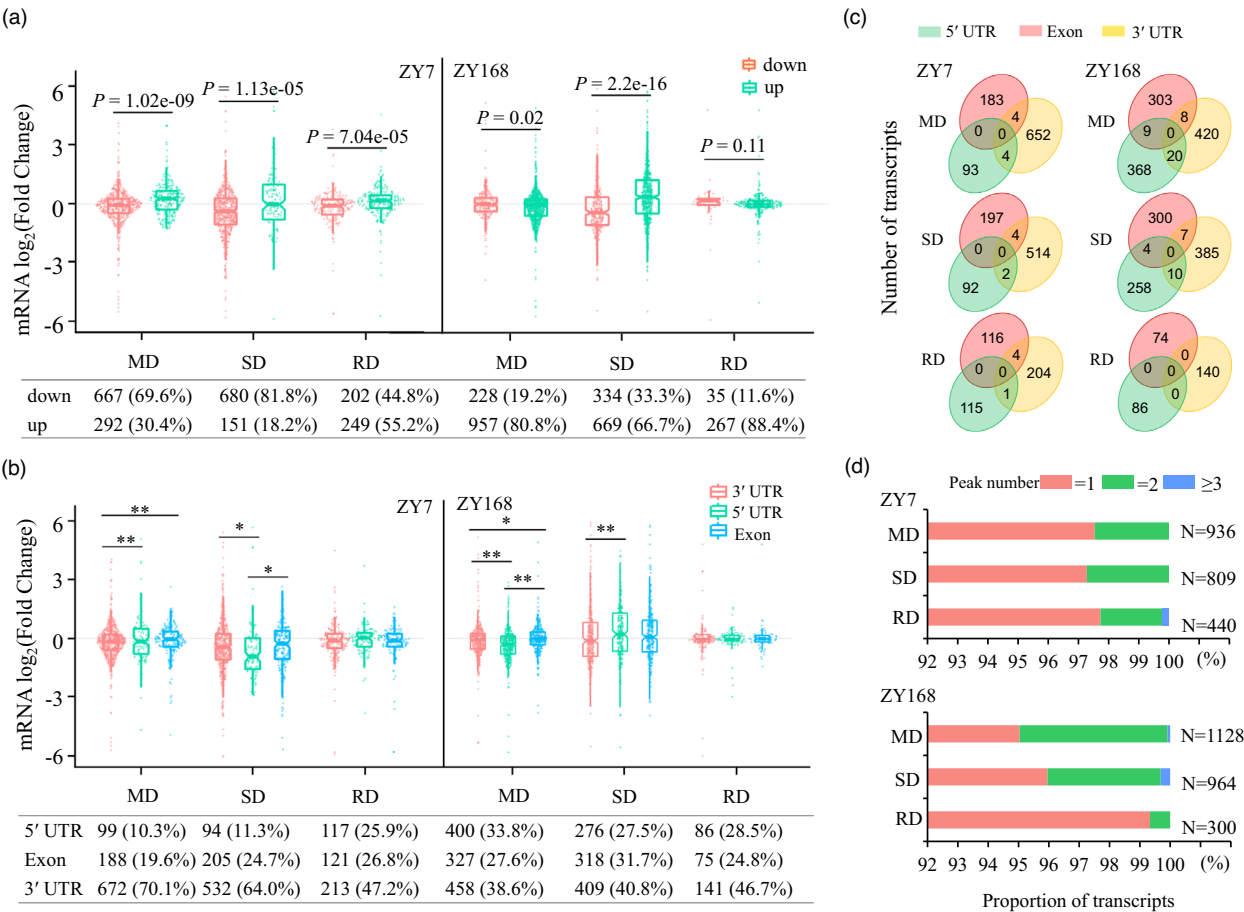


Figure 3 m^6A methylation affects the abundance of significant DMeTs under drought stress conditions. (a) Upregulated and downregulated significant DMeTs in ZY7 and ZY168 under mild drought (MD), severe drought (SD), and re-watering after drought (RD) conditions. The numbers in the bottom represent the number (proportion) of upregulated and downregulated significant peaks under each condition. (b) Distribution of the significant DMeTs in different genic regions (5'UTR, exon and 3'UTR) in ZY7 and ZY168 under different drought conditions. The numbers in the bottom represent the number (proportion) of significant peaks with m^6A methylated regions. Statistical significance was determined by Wilcoxon rank sum test: * $P < 0.05$, ** $P < 0.01$. (c) Venn plot for significant DMeTs of m^6A peaks in different regions in ZY7 and ZY168 under different drought conditions. (d) Proportion of transcripts with different numbers of significant m^6A peaks.

In these significant DMeTs, no single transcript could be identified that was simultaneously modified with m^6A at the 5'UTR, exon and 3'UTR. Most are modified with just one peak located in the 3'UTR, though a few were enriched with two peaks in the same region or two different regions (Figure 3c, d). The number of significant DMeTs with two peaks occurred under MD and SD rather than RD, and in ZY168 under RD that no two peaks could be found. It therefore suggested that drought affects the number of m^6A peaks in cotton.

Annotations of target genes with m^6A modification

We further screened the unique and common significant DMeTs with differentially methylated peaks in the two cotton varieties under different drought conditions. Firstly, ZY7 (677) and ZY168 (651) shared larger numbers of significant DMeTs under MD, and smaller numbers under RD (Figure 4a). While, 99, 70 and 235 common significant DMeTs were identified in both varieties under MD, SD and RD, which were the basic response of cotton plants to drought stress, with 837, 739 and 405 unique target transcripts identified in ZY7, and 1029, 894 and 265 unique

target transcripts identified ZY168. And for the same variety, 81 and 256 shared significant DMeTs was identified from MD to SD (under both MD and SD) and decreased to 31 and 62 after re-watering (under both SD and RD) in ZY7 and ZY168, respectively (Figure S7). The differentially expressed significant DMeTs (DMeETs) were obtained with the fold change (FC) in both m^6A enrichment (m^6A FDR < 0.05 , FC > 1.5) and mRNA expression level (mRNA FDR < 0.05 , FC > 2) for further analysis. It was found that only 8 DMeETs were enriched for m^6A modification and mRNA abundance in both ZY7 and ZY168, and 94 and 114 unique DMeETs were identified under MD for the representative varieties (Figure 4b). More DMeETs (20) were found in both varieties under SD, as well as 204 unique DMeETs identified in ZY7 and 299 in ZY168 (Figure 4c). As we described above, peaks decreased with re-watering after drought, and only one DMeETs (*Ghir_D08G013670.2*, *GhSAMS2*) was identified in both (Figure 4d), and the number of unique DMeETs decreased to 36 in ZY7 and 0 in ZY168. This suggests that homeostasis of m^6A modification on the transcript was not severely disrupted by drought stress.

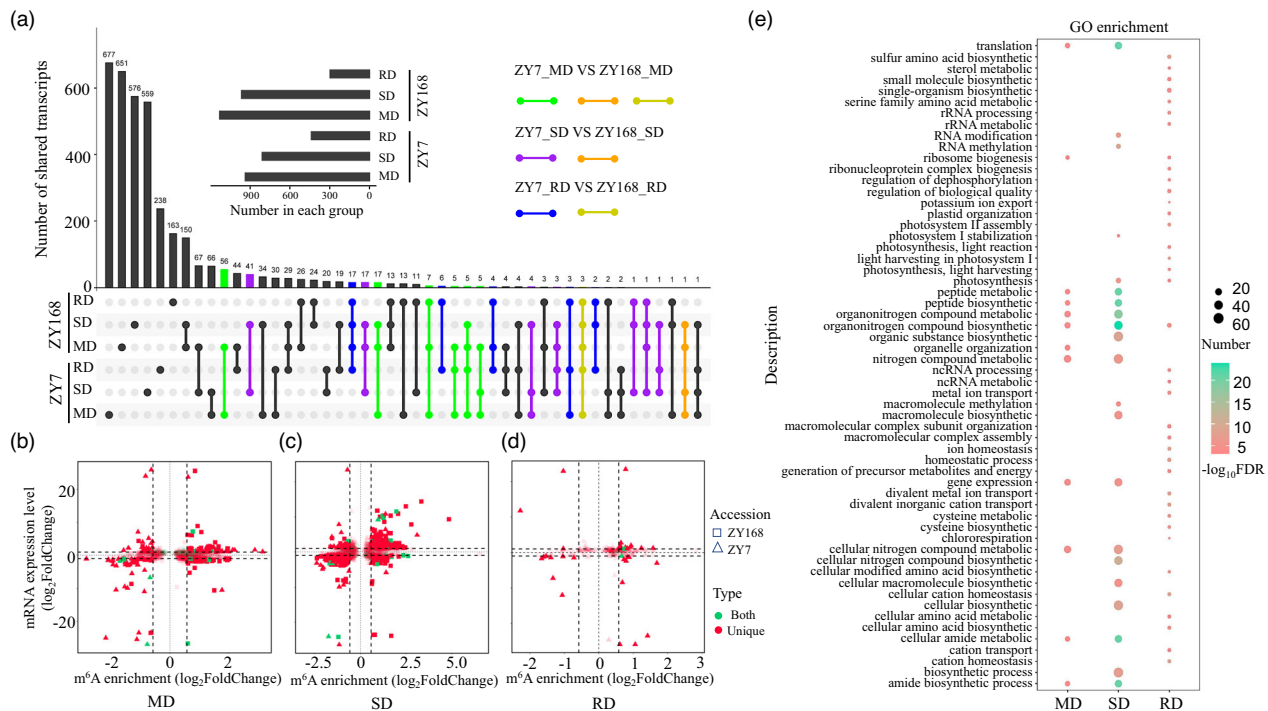


Figure 4 Annotation analysis of significant DMeTs and differentially expressed significant DMeTs (DMeETs) under drought stress conditions. (a) Upset plot for significant DMeTs between different samples. The sum of green, orange and yellow dot-lines represents the common significant DMeTs identified in both varieties under MD. The sum of purple and orange dot-lines represents the common significant DMeTs identified in both varieties under SD, and sum of blue and yellow dot-lines represents the common significant DMeTs identified in both varieties under RD. (b–d) Scatter plots for common and unique DMeETs under different drought conditions. Green fill represent common DMeETs identified in both varieties, red fill represent unique DMeETs identified in ZY7 (triangle) or ZY168 (square). (e) Gene ontology (GO) analyses of DMeETs in ZY7 under different drought conditions.

To further investigate the biological significance of DMeETs, gene ontology (GO) analysis was performed to uncover the biological functions of dynamic m⁶A regulation, except for ZY168 under RD due to insufficient DMeETs detected (Tables S6–S10), and we focused on biological processes that involved the methylated RNAs. DMeETs were annotated with GO terms in multiple biological processes, particularly in translation, RNA methylation, gene expression, and amide biosynthesis in both ZY7 (Figure 4e; Tables S6–S8) and ZY168 (Figure S8; Tables S9 and S10). These results suggest a role for m⁶A methylation in the biological response to drought stress by the regulation gene expression and translation through organonitrogen and ion transport pathways. Encyclopedia of Genes and Genomes (KEGG) analysis of these DMeETs was also performed. The most significant enriched pathways for these transcripts under drought were photosynthesis, carbon metabolism, porphyrin and chlorophyll metabolism, and pentose phosphate pathway, while cysteine and methionine metabolism, and amino acid biosynthesis were enriched after re-watering in both varieties (Figure S9; Tables S11 and S12). This indicates m⁶A modification is widely involved in and related to photosynthesis and carbon metabolism pathways in cotton.

GhALKBH10B is required for m⁶A modification during drought stress in cotton

The plant ALKBH protein family are demethylases responsible for RNA demethylation, and ALKBH9 and ALKBH10 are homologous to the mammalian ALKB homologous 5 (ALKBH5). In the current study, we identified 22 *ALKBH* homologous genes in the

allotetraploid upland cotton genome, including 4 *GhALKBH9* and 4 *GhALKBH10* gene members (Figure S10; Table S13). The homologous gene pair *GhALKBH10B-D* (Ghir_D08G007610) and *GhALKBH10B-A* (Ghir_A08G007520) was found to be predominantly expressed in vegetative organs, especially in root, stem and leaf. Another pair, *GhALKBH10A-D* (Ghir_D11G012740) and *GhALKBH10A-A* (Ghir_A11G012800), as well as homologous genes of *ALKBH9*, exhibit no obvious tissue specificity and are expressed at relatively low levels (Figure 5a). We further examined drought expression patterns of these *ALKBH* genes. *GhALKBH10B-D* and *GhALKBH10B-A* displayed significant expression changes during dynamic drought stress conditions, with up-regulation under drought, especially under SD, and down-regulation after re-watering (Figure 5b). *GhALKBH10A-D* and *GhALKBH10A-A* however maintained low expression levels from the beginning of drought application to re-watering in both accessions (Figure S11).

CRISPR-Cas9 gene editing technology was used to create the *alkbh10a*, *alkbh10b*, *alkbh9a* and *alkbh9b* mutant plants using two sgRNAs on each gene (Figure 5c; Figures S12 and S13). As a result, *alkbh10b* mutants with frame-shifted protein sequence (Figure S14) showed higher m⁶A/A ratios than WT under normal water condition, and even increased to relatively high levels under drought stress condition in LC–MS/MS assays (Figure 5d). We also detected the levels of m⁶A modification using m⁶A dot blots, which confirmed the m⁶A demethylase activity that the m⁶A levels was significantly increased in the *alkbh10b* mutants compared with WT (Figure 5e). Accordingly, *alkbh10b* mutants showed drought resistance phenotypes compared with WT for

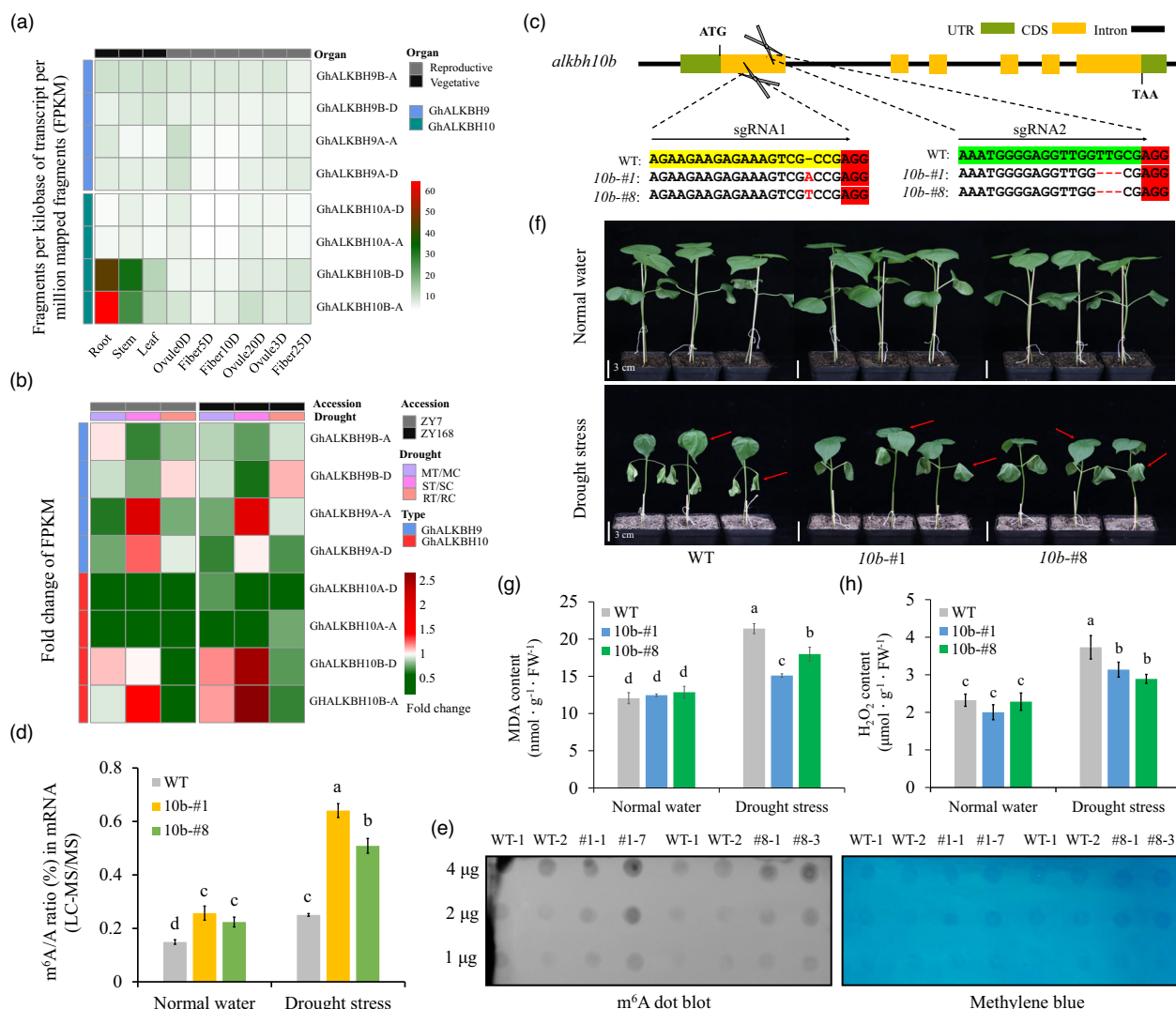


Figure 5 Characterizations of m^6A demethylase gene *GhALKBH10B*. (a) Tissue expression analysis for homologous genes *ALKBH9* and *ALKBH10* in *Gossypium hirsutum*. (b) Drought expression profiles for homologous genes *ALKBH9* and *ALKBH10* in ZY7 and ZY168. (c) Structural schematic diagram for constructing the mutant plants for *alkbl10b*. UTR, CDS and intron region was represented using darkgreen box, orange box and black line. Two scissors represented the designed sgRNAs, and within which "AGG" was the PAM location filled in red. (d) LC-MS/MS assay showing m^6A/A ratio in mutant plants under normal water and drought stress conditions. (e) RNA dot blot analysis of m^6A levels in the WT and *alkbl10b* using a specific m^6A antibody. Total RNA from the WT and the *alkbl10b* were extracted and spotted onto HybondTM-N+ membranes and incubated with an m^6A antibody, then detected using the enhanced chemiluminescence (ECL) detection system. Methylene blue staining served as a loading control. (f) Phenotype of mutant plants for *alkbl10b* and WT at seedling stage under normal water and drought stress conditions. *alkbl10b* showed lower wilting cotyledons and leaves (in red arrows) than WT under drought conditions. (g and h) MDA and H_2O_2 content for WT and *alkbl10a* plants under normal water and drought stress conditions. Error bars were calculated as SD based on at least three biological replicates, different lower-case letters a–d above columns represent significant differences among columns (Duncan's multiple comparisons, $P < 0.05$).

the withering cotyledons and leaves on WT plants (Figure 5f). Both malondialdehyde (MDA) and hydrogen peroxide (H_2O_2), two important physiological indices of cell damage under drought stress, were significantly lower in *alkbl10b* than WT after drought which indicated *alkbl10b* plants suffered lower degree of stress injury (Figure 5g, h). While, *alkbl10a* mutants also displayed higher m^6A/A ratios than WT under normal water condition, and also increased to high levels under drought stress condition, but without obvious phenotypic difference on drought resistance between mutant plants and WT plants (Figure S13). However, the m^6A/A ratios in *alkbl9a* and *alkbl9b* did not exhibit significant differences compared with WT, and no significant difference phenotype on drought resistance and

physiological indicators under drought stress (Figure S15). These results indicate that *GhALKBH10B* is an essential demethylase in cotton which might contribute to drought resistance. However, this does not prove that *GhALKBH9A* and *GhALKBH9B* has no RNA demethylation activity, since functional redundancy is common in the tetraploid cotton genome.

Genes in the ABA and Ca^{2+} signalling pathways exhibit differential m^6A methylation patterns during drought stress in cotton

We examined the regulatory function of *ALKBH10B* in drought response pathways with focusing on the enriched stress-responsive signal transduction pathways. Three transcripts,

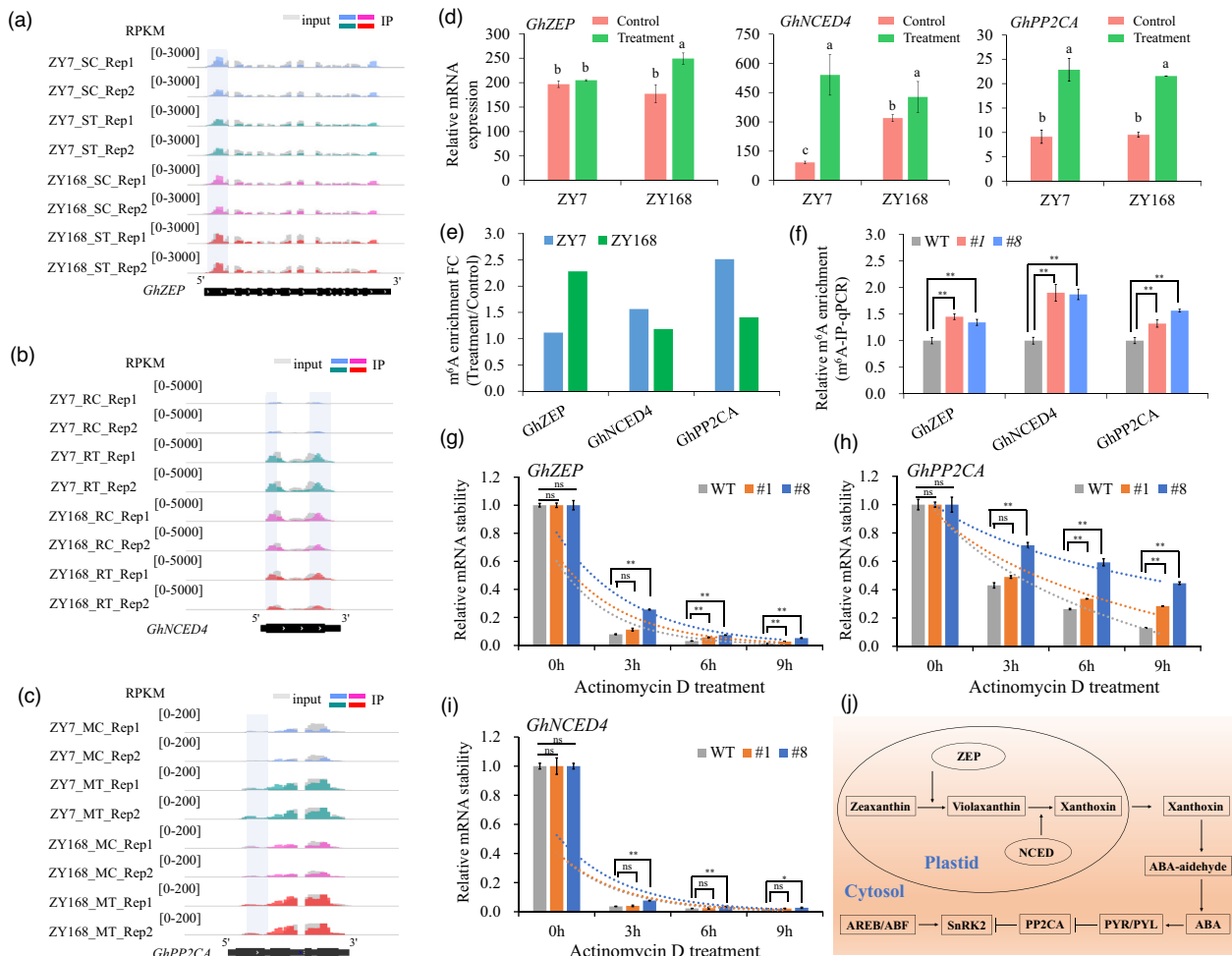


Figure 6 m⁶A modification facilitates mRNA stability of key genes in the ABA pathway during drought stress. (a–c), Integrative Genomics Viewer (IGV) tracks show *GhZEP*, *GhNCED4* and *GhPP2CA* identified by MeRIP-seq and mRNA-seq data. (d) Relative expression (FPKM) of *GhZEP*, *GhNCED4* and *GhPP2CA* under control or drought conditions in ZY7 and ZY168. Different lower-case letters a–d above columns represent significant differences among columns (Duncan's multiple comparisons, $P < 0.05$). (e) m⁶A enrichment fold change (FC) of *GhZEP*, *GhNCED4* and *GhPP2CA* identified by exomePeak. (f) m⁶A-IP-qPCR assay showing the relative m⁶A enrichment in wild type and mutant plants for *Ghalkb10b*. Error bars were calculated as SD based on three biological replicates, and statistical significance was determined by a two-sided *t*-test: ** $P < 0.01$. (g–i) Relative mRNA stability of *GhZEP*, *GhNCED4* and *GhPP2CA* in the wild type and mutant plants for *alkb10b*. (j) Diagrammatic representation of these three key genes in the ABA signalling pathway. Error bars represent SD of three biological replicates, statistical significance was determined by a two-sided *t*-test: * $P < 0.05$, ** $P < 0.01$. ns, no significance.

annotated as protein phosphatase 2C 37-like protein (PP2CA), 9-cis-epoxycarotenoid dioxygenase 4 (NCED4) and zeaxanthin epoxidase (ZEP) (ABA1) isoform 1, were enriched in the ABA biosynthesis and signalling pathway. Both *GhZEP* and *GhPP2CA* had an enriched m⁶A peak located in the 1st exon in IP samples under drought stress, and *GhNCED4* had an enriched peak located in both first exon and 3'UTR (Figure 6a–c). The expression levels of these three genes were upregulated under drought stress in both varieties or at least in one variety (Figure 6d), indicating that at least some ABA-related genes are induced by drought stress. At the same time, the m⁶A enrichment of these three genes was also upregulated under drought condition compared to watered control, but with different fold change for different genes in either ZY168 or ZY7 (Figure 6e). For instance, *GhZEP* was significantly upregulated in mRNA expression and m⁶A enrichments in ZY168, while no significance been observed in ZY7. The expression of

GhNCED4 was significantly upregulated in both varieties with little difference between ZY7 and ZY168. The expression of *GhPP2CA* was also significantly upregulated in both varieties but only showing significance of m⁶A enrichment in ZY7 under control and drought condition. (Figure 6d, e).

We further confirmed that these three ABA-related genes exhibited relatively higher levels of m⁶A enrichment in *alkb10b* plants than control, both in *alkb10b*-#1 and *alkb10b*-#8 (Figure 6f), but only *GhPP2CA* presented higher levels in *alkb10a* than WT (Figure S17). To better understand how m⁶A methylation affects transcript abundance, we investigated the mRNA stability of *GhZEP*, *GhPP2CA* and *GhNCED4* by calculating the mRNA degradation rate using actinomycin D to inhibit transcription. It was seen that mRNA degraded after 3 h treatment, and the degradation rate decreased for mRNAs of *GhZEP* and *GhPP2CA* in *alkb10b* mutant plants (Figure 6g, h), but only a little difference was seen for *GhNCED4* in *alkb10b*-#8 (Figure 6i).

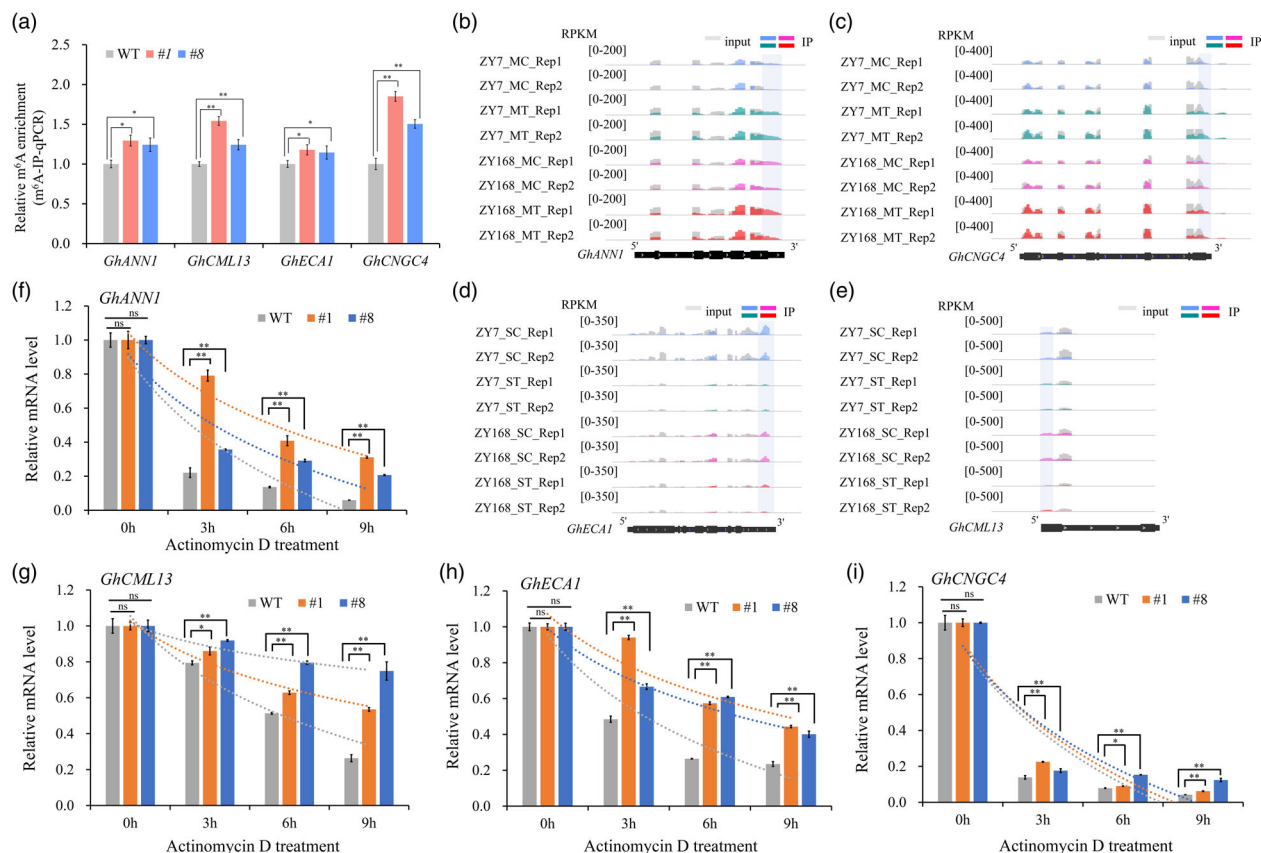


Figure 7 m⁶A modification facilitates mRNA stability of key genes in the Ca²⁺ signalling pathway during drought stress. (a) m⁶A-IP-qPCR assay showing the relative m⁶A enrichment of Ca²⁺-related genes (*GhANN1*, *GhCML13*, *GhECA1* and *GhCNGC4*) in wild type and mutant plants for *alkbh10b*. Error bars represent SD of three biological replicates, statistical significance was determined by a two-sided *t*-test: * *P* < 0.05, ** *P* < 0.01. (b-e) IGV tracks showing *GhANN1*, *GhCML13*, *GhECA1* and *GhCNGC4* identified by MeRIP-seq and mRNA-seq data. (f-i) Relative mRNA stabilities of *GhANN1*, *GhCML13*, *GhECA1* and *GhCNGC4* in wild type and mutant plants for *alkbh10b*. Error bars represent SD of three biological replicates, statistical significance was determined by a two-sided *t*-test: * *P* < 0.05, ** *P* < 0.01. ns, no significance.

Concomitant with m⁶A deposition in the mutant plants, m⁶A slowed down degradation and therefore stabilized mRNAs for these key ABA-related genes (Figures 6j and S16).

We also identified some DMeTs related to Ca²⁺ signal transduction. *GhANN1* (cotton annexin D1), *GhCML13* (Probable calcium-binding protein CML13), *GhECA1* (Calcium-transporting ATPase 1, endoplasmic reticulum-type-like protein), and *GhCNGC4* (Cyclic nucleotide-gated ion channel 4-like protein) were confirmed to be enriched in m⁶A modification in both *Ghalkbh10b*-#1 and *Ghalkbh10b*-#8 plants (Figure 7a), but only *GhECA1* and *GhCNGC4* showed higher m⁶A levels in *alkbh10a* than WT (Figure S17). The methylated regions were in the 3'UTR of these genes except for *GhCML13*, where it was located in the 1st exon near to the 5'UTR (Figure 7b-e). The stability of these genes' mRNA was also significantly increased in knockout plants under actinomycin D treatment, similar to the findings for ABA-related genes (Figures 7f-i and S16). These results suggest that GhALKBH10B contributes to mRNA stability of genes in the Ca²⁺ and ABA signalling pathways.

Defective expression of m⁶A-targeted Ca²⁺ signal related genes affects drought resistance in cotton

Further functional validation of the m⁶A targeted Ca²⁺ signal related genes was carried out by virus-induced gene silencing

(VIGS) technology. *GhECA1* and *GhCNGC4* were two key genes involved in Ca²⁺ signal pathway in response to drought that *GhECA1* was downregulated and *GhCNGC4* was upregulated under drought stress in two varieties (Figure S18). By applying drought stress to the seedlings, plants silenced for TRV::*GhECA1* and TRV::*GhCNGC4* exhibited earlier wilting compared to controls (TRV::00; Figure 8a, b) with the decreased m⁶A enrichment on silenced genes (Figure 8c). PD₆, a well-illustrated image-based trait, which could indicate the drought ability of cotton plants with high value presenting lower drought resistance ability in our previous paper (Li et al., 2020), was significantly higher than that of control plants (Figure 8d). Meanwhile, both MDA and H₂O₂ showed significant increases in the silenced TRV::*GhECA1*, TRV::*GhCNGC4* and TRV::00 plants under drought compared to controls (Figure 8e, f). Moreover, the roles of these two genes in mediating calcium ion flow were further investigated by Non-invasive Micro-test Technology (NMT). Ca²⁺ flux direction was changed in the mesophyll cells of silenced plants, and specific Ca²⁺ exhibited efflux in silenced plant while controls retained influx after drought stress, despite a higher influx than in normal water conditions (Figure 8g), which also indicated the decreasing drought resistant in silenced plants. This demonstrates the positive regulatory functions of *GhECA1* and *GhCNGC4* in the drought response.

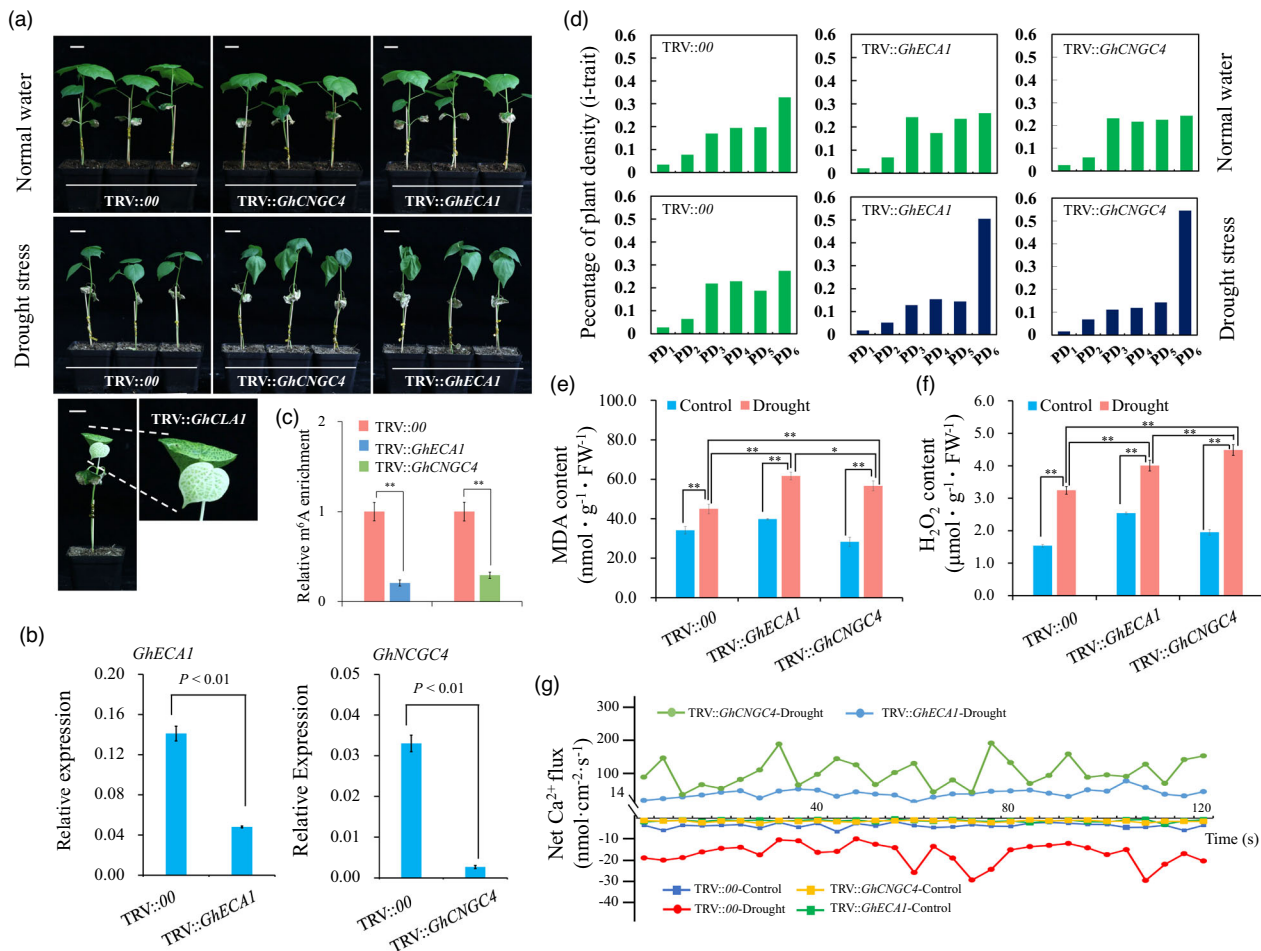


Figure 8 GhECA1 and GhCNGC4 positively regulate drought tolerance in cotton. (a) Virus-induced gene silencing (VIGS) assay for *GhECA1* and *GhCNGC4* under drought stress condition (absolute soil water content, ASWC = ca. 12.7%). TRV::00 (empty vector) was the blank control panel, and TRV::GLA was the reference for gene silencing with an albino phenotype. (b) Relative expression of *GhECA1* and *GhCNGC4* in silenced plants and control TRV::00. (c) Relative m⁶A enrichment on *GhECA1* and *GhCNGC4* in silenced and control plants. (d) The percentage of plant density (image-based traits, i-trait) for gene silenced plant (TRV::GhECA1 and TRV::GhCNGC4) and empty vector plant under normal water and drought stress conditions. The plant density PD₁₋₆ stood for the ratio of six shading degrees from lowest to highest, respectively. (e-f), MDA and H₂O₂ content in TRV::00, TRV::GhECA1 and TRV::GhCNGC4 plants under control and drought treatments. Drought was measured by absolute soil water content (ASWC = ca. 12.7%) by a manual weighing method. Error bars represent SD of three biological replicates, statistical significance was determined by a two-sided *t*-test: * *P* < 0.05, ** *P* < 0.01. (g) Non-invasive Micro-test Technology (NMT) for Ca²⁺ flux over 120 s. Negative value represents Ca²⁺ influx and positive value represents Ca²⁺ efflux. TRV::00-Control represents TRV::00 under normal water conditions, and TRV::00-Drought for plants under drought conditions.

Discussion

Drought response is highly regulated at the genomic and transcriptional levels (Gupta *et al.*, 2020; Wang *et al.*, 2016a). Due to the complexity of cotton genome (Chen *et al.*, 2020), the drought response mechanism in cotton is poorly defined compared with food crops such as rice, maize and wheat. Previously identified changes in transcription and epigenetic modification during drought stress have greatly improved our understanding of the mechanism related to cotton drought response (Li *et al.*, 2020; Liang *et al.*, 2016; Liu *et al.*, 2014a; Shang *et al.*, 2020). In the present study, we show that a considerable number of mRNAs exhibit drought-regulated methylation, with differential levels of m⁶A modification under drought stress in both drought-resistant and drought-sensitive varieties (Figure 1). These observations suggest that m⁶A

modification might be another important contributor to the drought response mechanism.

The overall m⁶A levels was slightly increased under mild drought condition (MD), but significantly increased under severe drought conditions (SD), up to the point of recovery following re-watering (RD), both in drought-resistant and drought-sensitive varieties; these are different to what reported in maize and sea buckthorn (Miao *et al.*, 2020; Zhang *et al.*, 2021). Moreover, drought triggered different m⁶A modifications in drought-resistant versus drought-sensitive varieties under different drought conditions. m⁶A peaks were enriched mostly in the 3'UTR in cotton (with the proportion > 60%), consistent with previous reports in other plants (Zhang *et al.*, 2019; Zheng *et al.*, 2021; Zhou *et al.*, 2022). The drought-sensitive variety ZY7 exhibited a similar proportion of m⁶A modification under MD and SD. While, the distribution of m⁶A modification changed

dramatically, with the enrichment of m⁶A near the 5'UTR region increasing significantly in drought-resistant variety ZY168 under MD and SD (Figure 2c). Accordingly, we identified more transcripts within 5'UTR deposited m⁶A peaks in drought-resistant variety ZY168 (762 peaks on 594 transcripts) than in drought-sensitive variety ZY7 (310 peaks on 288 transcripts) (Tables S4 and S5).

GO and KEGG analyses revealed that numerous genes regulating ion transport, photosynthesis, or carbon metabolism acquire m⁶A marks in a drought-dependent manner, with the expression of 748 genes under tight regulation by their methylation status (Table S14). We found that some genes related to stress response and signalling, including ABA biosynthesis and signalling and Ca²⁺ transport and signalling genes, undergo m⁶A-mediated post-transcriptional regulation during drought response in cotton. In the seven genes we selected, four genes (*GhZEP*, *GhPP2CA*, *GhNCED4* and *GhCML13*) harboured m⁶A site near the 5'UTR (in the 5'UTR or in the 1st exon), with three genes (*GhZEP*, *GhNCED4* and *GhCML13*) harbouring cotton specific CAAUG motif. The m⁶A levels of these genes increased in *alkbh10b* plants compared to the control. Increased m⁶A abundance is known to improve mRNA stability for some key stress-responsive genes in Arabidopsis (Anderson et al., 2018), sorghum (Zheng et al., 2021) and apple (Hou et al., 2022). Meanwhile, there also appears to be a complex relationship between the positions of m⁶A peaks in RNAs and their abundance, with positive relations in mRNA levels with m⁶A modification regulated by water conditions either in drought-sensitive or drought-resistant varieties. The m⁶A modification for *GhNCED4* was both enriched in the 5'UTR and 3'UTR region, while the peak was in the 1st exon close to the 5'UTR for *GhZEP* and *GhPP2CA*. These genes showed upregulated 5'UTR m⁶A modification, which was accompanied by up-regulation of mRNA levels under drought stress (Figure 6). While, downregulated 5'UTR m⁶A modification of *GhCML13* resulting in the down-regulation of mRNA levels (Figure 7). The m⁶A modification for *GhCNGC4*, *GhECA1* and *GhANN1* was mainly enriched in the 3'UTR region, with upregulated m⁶A modification of *GhCNGC4* and *GhANN1* linked to the up-regulation of m⁶A levels after drought stress (Figure 7). These results indicate that the different distributions of m⁶A modification under different water conditions in different varieties, which might contribute to the different ability of drought resistance in different cotton varieties, and this was not reported in any other study.

The dynamic RNA methylation levels during drought stress in cotton reveal its importance to maintain the balance of RNA methylation under drought stress, which is accomplished by both m⁶A methyltransferases and demethylases. Understanding the functional roles of reversible m⁶A methylation in mammals has been paramount since the discovery of the first human mRNA m⁶A demethylase FAT MASS AND OBESITY-ASSOCIATED (FTO) (Jia et al., 2011). In Arabidopsis, there are 13 potential RNA demethylases, among which *ALKBH10B* functions in floral transition by regulating the methylation of key flowering-related mRNAs for *FT*, *SPL3* and *SPL9* (Duan et al., 2017), while *ALKBH9B* modulates infection by alfalfa mosaic virus (Martinez-Perez et al., 2017) and *ALKBH6* functions in growth and stress responses (Huong et al., 2020). There are fewer RNA demethylases elucidated in other plants. Tomato DNA methylation-dependent RNA demethylase *SIALKBH2* functions in fruit ripening by regulating the abundance of *SIDML2* mRNA (Zhou et al., 2019). *ZmALKBH10* was induced by drought stress and acts to decrease m⁶A abundance in maize (Miao et al., 2020). A search of the

upland cotton genome led to the identification of 22 homologous *ALKBH* genes (Table S13). Gene expression analysis indicated that the expression of *GhALKBH10B* increases dramatically after drought stress in cotton, which was consistent with the reported in maize and sea buckthorn (Miao et al., 2020; Zhang et al., 2021). However, there was unharmony that the overall methylation level also increased after drought stress in cotton, implying the complexity in studying m⁶A in response to drought, potentially due to be co-regulated by methyltransferases.

Consequently, RNA m⁶A methyltransferase is another important factor for the maintenance of RNA methylation at appropriate levels (Chen et al., 2018; Lu et al., 2020; Pendleton et al., 2017; Zhang et al., 2019; Zhou et al., 2021). Recently, MdMTA was reported to enhance drought tolerance by increasing m⁶A modification on drought-responsive genes in apple by using overexpression and RNAi technologies (Hou et al., 2022). Here, 6 homologous *METTL3* (*AtMTA*) genes and 2 homologous *WTAP* (*AtFIP37*) genes were identified in upland cotton genome (Table S15). We created mutant plants of the homologous methyltransferase genes (*GhMTA* and *GhFIP37*) in cotton, but the T₀ generation of knockout transgenics (*mta* and *fip37*) grew weakly and exhibited abnormal reproductive growth, with poor seed set, and even unbolling (Figure S19), which was consisted with their functions in reproductive development in rice (Zhang et al., 2019). Dose-dependent mutation by manipulating on promoters was needed for further study.

Rapid advances have been made in understanding the functional diversity and regulatory mechanisms of m⁶A marks on abiotic stress response in plants. In the recent study, we generated a transcriptome-wide m⁶A map in cotton and uncovered the dramatic patterns of m⁶A modifications associated with drought response using MeRIP-seq data in cotton. We propose the regulatory role of m⁶A methylation in drought response of cotton by targeting some vital stress-related genes such as genes in Ca²⁺ and ABA signalling pathways. Our study corroborated and complemented the conclusion that RNA methylation facilitates mRNA stability contribute to drought resistance as reported in apple and other plants, and even better to confirmed function of m⁶A on the stability of Ca²⁺ and ABA signalling pathway related genes mediated by *GhALKBH10B*. Other than the rough map in other studies, we used different water condition and varieties with different drought resistant ability to generate the global map. We highlight that increasing of m⁶A enrichment near the 5'UTR region under drought stress in drought-resistant variety might contribute to the different ability of drought resistance of different cotton varieties. Moreover, this study not only expended our understanding of *ALKBH10B* functioned with affecting floral transition in Arabidopsis, but also provides new insights into the drought response network as well as new strategy for drought resistance breeding of cotton. Both writers and erasers had the global impact on whole transcriptome, and knock out them using CRISPR/Cas9 could lead to changes in m⁶A modification on many transcripts. Future research should focus on site-specific m⁶A modifications of targeted mRNA, which could precisely decipher the regulated mechanism of m⁶A in diversiform biological process.

Methods

Cotton materials and drought stress treatments

Drought experiments were carried out using two representative cotton varieties of drought-resistant ZY168 and drought-sensitive

ZY7 as our previous study (Li *et al.*, 2020). Germinated cotton seedlings were planted in pots filled with mixed nutrient soil in the greenhouse. Drought stress was imposed by withholding water supply continuously after the first leaf had fully spread, at three time-points, that is, mild drought (MD), severe drought (SD), and re-watering after drought (RD). Absolute soil water content (ASWC) was used to evaluate the different drought degrees at these time-points. At the beginning of the experiment, the weight of dry mixed nutrient soil (4.5 kg) and pot (0.2 kg) was 4.7 kg for each. To record the ASWC during the growth of cotton, the whole weight (WW1) including pot and soil was weighed every day. The ASWC (%) was calculated as $(WW1 - 4.7) / 4.5 \times 100$. And the ASWC at ca. 10% for MD, at ca. 5% for SD, ASWC and at ca. 15% for RD. At the same time, a parallel control panel with normal water supply was maintained at an ASWC of ca. 15% at each point. Newly emerged second true leaves were sampled and mixed at MD, SD and 6 days after RD. Leaf samples were obtained at the same time (11:00 am), immediately frozen in liquid nitrogen, and stored at -80°C until sequencing.

Global m⁶A quantification by LC–MS/MS

Total RNA was extracted from the leaves of drought-treated and parallel control cotton plants under MD, SD and RD conditions using the TG-DP441 RNA Kit (TIANGEN, Beijing, China) following the manufacturer's procedure. The quality and quantity of total RNA were analysed using a Bioanalyzer 2100 and RNA 6000 Nano LabChip Kit (Agilent, CA, USA) with RIN number >7.0.

The total m⁶A/A ratio in cotton was determined by LC–MS/MS as previously described (Zhou *et al.*, 2019) with minor modifications. mRNA was isolated from total RNA using Dynabeads Oligo (dT)₂₅ (Invitrogen, 61 006). 200 ng was digested to 5'-mononucleotides with 1 unit of Nuclease P1 (NEB, M0660S) in 50 μL reaction buffer (10 mM ammonium acetate, pH 5.3, 25 mM NaCl, and 2.5 mM ZnCl₂) for incubation at 37°C for 6 h. Then the reaction product was mixed with 1 unit of alkaline phosphatase (Sigma-Aldrich, P6774-1) and 5 μL 1 M fresh NH₄HCO₃, and incubated at 37°C for another 6 h. The supernatant of digested sample was collected and diluted to a suitable concentration for LC–MS/MS assay following a published method (Zhou *et al.*, 2018) with minor modifications. In brief, nucleoside standards including N⁶-methyladenosine and adenosine nucleoside were used to determine the peak position of each nucleoside. Nucleosides were separated by reverse-phase ultra-performance liquid chromatography on a C18-ODS column (Shimadzu). The AB SCIEX Triple Quad 5500 System liquid chromatography mass spectrometer was used for online mass spectrometry detection, set to multiple reaction monitoring in positive electrospray ionization mode. The mobile phase consisted of buffer A (5 mM ammonium acetate) and buffer B (100% acetonitrile). Nucleosides were quantified using the nucleoside-to-base ion mass transitions of 282.0–150.1 (m⁶A) and 268.0–136.0 (A). Standard curves were generated by running a concentration series of pure commercial A (TargetMol, T0853) and m⁶A (TargetMol, T6599). Quantification was determined by comparison with the standard curves obtained from nucleoside standards running at the same time. Three independent biological replicates were performed for each sample.

MeRIP-seq, mRNA-seq and data analysis

The MeRIP-seq was based on a previously described method with minor modifications (Dominissini *et al.*, 2013). Briefly, mRNA was

purified by poly-T oligo, then fragmented and constrained input and IP libraries for sequencing through Illumina Novaseq™ 6000 platform. The detailed method for MeRIP-seq and related data analysis was supplied in Method S1.

Creation for mutants of demethylase genes

Blastp (identity >40%, e-value <1e-30, score > 150) was used to identify homologous m⁶A methylases in upland cotton TM-1 (Wang *et al.*, 2019). A phylogenetic tree was constructed using protein sequences with the software MEGA-X (Kumar *et al.*, 2013) with the Tets-Neighbour-Joining method, and the calculated result was exported to iTOL (<http://itol.embl.de/>) for drawing.

CRISPR-Cas9 gene editing technology was used to construct vector for *GhALKBH9A* (*Ghir_A04G014040*), *GhALKBH9B* (*Ghir_D11G018740*), *GhALKBH10A* (*Ghir_D11G012740*) and *GhALKBH10B* (*Ghir_D08G007610*), using published procedures (Wang *et al.*, 2018). In brief, targets sequences were searched from the CRISPR-P website (<http://cbi.hzau.edu.cn/crispr/>), and each pair of sgRNAs, named sgRNA1 and sgRNA2, were designed to be integrated in a demethylase vector. Fragments containing tRNA-sgRNA1 fusion and gRNA-tRNA-sgRNA2 fusion amplified from pGTR plasmid were fused together using an overlapping extension PCR. The tRNA-sgRNA1-gRNA-tRNA-sgRNA2-gRNA assembled fragments were finally ligated to the linearized pRGE32-NPT II-U6.7 vector for creating demethylase knockout vectors. The primers used in vector construction are listed in Table S16. All the constructed plasmids were separately introduced into *Agrobacterium tumefaciens* strain GV3101 by electroporation. The hypocotyls of wild-type cotton (Jin668) cultured in a 28°C incubator for approximately 7 days were cut into stem segments of 0.5–0.8 cm, and were used transferred into the activated *agrobacterium tumefaciens*. After 3–5 min of infection, the hypocotyls were dried slightly, placed on the co-culture medium with filter paper for 36 h at 20°C . And then cultured on the selective medium containing appropriate antibiotics until embryogenic callus grows, which were then selected into the differentiation medium to make it grow into embryoids, and then develop into transgenic cotton seedlings. The cotton genetic transformation method is as described previously (Jin *et al.*, 2006). Mutants were detected using the published Hi-TOM program (Liu *et al.*, 2019).

m⁶A-IP-qPCR

Total RNA was extracted from leaves in WT (Jin668) and mutant plants (*alkbh9a*, *alkbh9b*, *alkbh10a* and *alkbh10b*) at 28 days after seed germination. mRNA was isolated from total RNA using Dynabeads Oligo(dT)₂₅ (Invitrogen, 61 006) according to the kit instructions. 2 μg poly(A)⁺ mRNA was randomly fragmented into ~300 nt long fragments by an incubation at 94°C for 30 s in fragmentation buffer, and the reaction terminated by addition of EDTA, followed by phenol-chloroform extraction and ethanol precipitation to purify the fragmented mRNAs according to Zhou *et al.* (2019). Fragmented mRNA was precipitated and resuspended in 150 μL RNase-free water. NanoDrop spectrophotometry was used to measure concentrations of fragmented mRNA, and fragmented mRNA size was validated in a 1.5% (wt/vol) agarose gel (Figure S20). 10 μL fragmented mRNA was retained and used as the input sample (control). 100 μL fragmented mRNA was incubated with 5 μg m⁶A-specific antibody at 4°C for 2 h, which was later used to perform MeRIP experiments according to the instructions for the Magna MeRIP m⁶A Kit

(Merck, A-17-10 499). Fold enrichment of the specific region of transcripts was determined by qRT-PCR using $2^{-\Delta CT}$ methodology, the value of ΔCT (cycle threshold) was normalized by ΔCT_{IP} , ΔCT_{input} and input dilution factor. The designed primers for m⁶A-IP-qPCR were shown in Table S16. Statistical significance was determined by a two-sided *t*-test on three biological replicates: **P* < 0.05, ***P* < 0.01.

Dot blot assay

Dot blot assay was performed as described previously with minor modifications (Ren et al., 2022). Total RNA from the WT and the *alkbh10b* mutant were extracted and heated at 95 °C for 5 min to remove the secondary structure and then was chilled on ice. RNA was spotted onto Hybond™-N+ membrane. The membrane was crosslinked using an HL-2000 HybriLinker for 5 min and then washed with TBST (TBS with Tween-20) for 5 min to remove the unbound RNA and blocked in 5% non-fat milk for 1 h at room temperature. The membrane was then incubated with an m⁶A antibody (1:2000; ABClonal) overnight at 4 °C. The membrane was washed using TBST and incubated with the secondary antibody for 1 h at room temperature. Finally, the super ECL detection reagent (Yeasten) was used for visualization.

Transcription inhibition assay

The procedure is based on the previously described method (Duan et al., 2017) with minor modifications. Briefly, 28-d-old cotton leaves of wild type (Jin668) and mutant plants (*alkbh10b-#1* and *alkbh10b-#8*) were cut into leaf discs and then added to actinomycin D (AbMole, M4881) solution with a final concentration of 20 µg mL⁻¹. After infiltration for 1 h, five leaf disks were collected and considered as time 0 controls, and subsequent samples were harvested every 3 h in triplicate, and qRT-PCR conducted with ABI 7500 system (Applied Biosystems, Foster city, CA) was used to determine mRNA expression levels, with the internal control *GhUBQ7*. The $2^{-\Delta CT}$ method was used to present relative changes in gene expression levels (Schmittgen and Livak, 2008). The mRNA degradation was calculated by the percentage of gene expression at sampled time relative to control. All primers used in transcription inhibition assay are listed in Table S16.

Drought treatments for mutant lines, VIGS assay, and functional analysis

Drought stress was imposed to the seedlings of generation T₂ of mutant lines (*alkbh10a-#2*, *alkbh10a-#3*, *alkbh10b-#1*, *alkbh10b-#8*, *alkbh9a-#4* and *alkbh9b-#1*) by withholding water supply continuously after 10 days post germination in an environments controlled chamber (CONVIRON, MTR30-190316) at temperature of 28–30 °C with 16 h light and 8 h dark (30% humidity, 100 µMol multi-chip LED lights) for growing and natural drought treatment. The phenotypes and physiological indices were taken at time of the ASWC (%) at about 12% in treatment panels. At the beginning of experiment, all cotton seeds were sown in the same pot (55 g nutrient soil and 15.4 g pot) with saturated water in a same big container. The whole weight (WW2) including pot and soil was weighed every day. The ASWC (%) was calculated as (WW2-70.4) / 55 × 100. Physiological indices of MDA and H₂O₂ were measured by kits provided by COMIN Technology CO., Ltd. (Suzhou, China), 4–5 seedlings were pooled for each biological replicate and at least three biological replicates were measured in experiments. Statistical

significance was determined by a two-sided *t*-test on three biological replicates: **P* < 0.05, ***P* < 0.01.

Virus-induced gene silencing (VIGS) technology was used to verify the function of m⁶A modified transcripts under drought treatment in cotton. The procedure of VIGS was based on a previous method (Gao et al., 2013). 300–500 bp fragment of the target gene (*GhECA1* or *GhCNGC4*) was cloned into the pTRV2 vector, and pTRV2 vector (empty vector) without target gene was used as a control. Both vectors were transformed into *A. tumefaciens* GV3101 by electroporation. Agrobacterium solution containing pTRV1 or pTRV2 vectors was cultured overnight in liquid LB medium with kanamycin 50 mg/L and rifampicin 25 mg/L, and collected by buffer solution (10 mmol/L MES, 10 mmol/L MgCl₂, 40 µg/mL AS, pH 5.6) and resuspended and adjusted to OD₆₀₀ of 0.6–0.8, then pTRV1 and pTRV2 (TRV:*GhECA1* or TRV:*CNGC4*) were mixed in equal quantities and placed in a 28 °C shaker at 150 r/min for activation for 2 h, before agroinfiltration into the cotyledons of Jin668 by syringe inoculation when the two cotyledons had fully spread (12 days after sowing). TRV:*CLA1* (*GhCLA1*, a key enzyme for chloroplast synthesis) plants were used as a positive control. After covering with black plastic film (removed after 24 h), these inoculated plants were placed to the controlled chamber, at temperature of 25 °C, light and humidity was the same to drought treatment described above. Then, watering to saturation for the initiation of natural drought treatment. The phenotypes and physiological indices of MDA and H₂O₂ were analysed at the time of the ASWC at about 12.7%. The image-based traits were extracted for the images followed our previous methods (Li et al., 2020).

Ca²⁺ flux assay with non-invasive micro-test technology

Net Ca²⁺ flux of mesophyll cells was measured using NMT (NMT-YG-100; Younger USA, Amherst, MA, USA) as previously described with minor modifications (Li et al., 2021). Leaves sampled from cotton following VIGS were immobilized in the measuring buffer (0.1 mM KCl, 0.1 mM CaCl₂, 0.1 mM MgCl₂, 0.5 mM NaCl, 0.3 mM MES, 0.2 mM Na₂SO₄, pH 6.5) for 10 min to recover from mechanical damage, and the steady-state ion fluxes in leaf mesophyll cells were then continuously recorded for the indicated times at room temperature. During measurements, the ion microsensor was placed about 3 µm above the surface of a cell and moved repeatedly between two points (10 µm in distance) perpendicular to the cell (Figure S21). The results of net Ca²⁺ ion fluxes were calculated by imFluxes V2.0 software (YoungerUSA LLC, Amherst, MA).

Author contributions

XY, XZ and XN designed and guided the project. KL and MW gave comments on the project. BL and MZ performed experiments and wrote the manuscript. BL and BZ carried out the drought treatment experiments. DY help creating the mutants plants. WS help performing the NMT experiments. LD help extracting imaging traits. BL and YM analysed the data. XY, KL and XZ revised the manuscript.

Acknowledgements

We thank Hongbo Liu (National Key Laboratory of Crop Genetic Improvement, Huazhong Agricultural University) for technical assistance with the LC-MS/MS assay. We also thank LC-Bio

Technology CO., Ltd. (<http://www.lc-bio.com/>) for the assistance with MeRIP-seq assay.

Funding

This work was supported by grants from the National Natural Science Foundation of China (32201725 and 32171942), the Bintuan Science and Technology Program (2022DB012), the Natural Science Foundation of Hubei Province (2022CFB756), the China Postdoctoral Science Foundation (2022M711279) and Fundamental Research Funds for the Central Universities (2662020ZKPY011).

Conflict of interest Statement

The authors declare that they have no competing interests.

Data Availability statement

The raw sequencing data were uploaded and deposited in NCBI (<https://www.ncbi.nlm.nih.gov/bioproject/PRJNA755074>).

References

- Anderson, S.J., Kramer, M.C., Gosai, S.J., Yu, X., Vandivier, L.E., Nelson, A.D.L., Anderson, Z.D. *et al.* (2018) N(6)-Methyladenosine inhibits local ribonucleolytic cleavage to stabilize mRNAs in Arabidopsis. *Cell Rep.* **25**, 1146–1157.
- Arribas-Hernandez, L., Bressendorff, S., Hansen, M.H., Poulsen, C., Erdmann, S. and Brodersen, P. (2018) An m(6)A-YTH module controls developmental timing and morphogenesis in Arabidopsis. *Plant Cell* **30**, 952–967.
- Cantara, W.A., Crain, P.F., Rozenski, J., McCloskey, J.A., Harris, K.A., Zhang, X., Vendeix, F.A. *et al.* (2011) The RNA modification database, RNAMDB: 2011 update. *Nucleic Acids Res.* **39**, D195–D201.
- Chen, M., Wei, L., Law, C.T., Tsang, H.C., Shen, J., Cheng, L.H., Tsang, L.H. *et al.* (2018) RNA N6-methyladenosine methyltransferase-like 3 promotes liver cancer progression through YTHDF2-dependent posttranscriptional silencing of SOCS2. *Hepatology* **67**, 2254–2270.
- Chen, Z.J., Sreedasyam, A., Ando, A., Song, Q.X., De Santiago, L.M., Hulse-Kemp, A.M., Ding, M.Q. *et al.* (2020) Genomic diversifications of five *Gossypium* allopolyploid species and their impact on cotton improvement. *Nat. Genet.* **52**, 525–533.
- Cheng, Q., Wang, P., Wu, G., Wang, Y., Tan, J., Li, C., Zhang, X. *et al.* (2021) Coordination of m⁶A mRNA methylation and gene transcriptome in rice response to cadmium stress. *Rice* **14**, 62.
- Dittrich, M., Mueller, H.M., Bauer, H., Peirats-Llobet, M., Rodriguez, P.L., Geilfus, C.M., Carpentier, S.C. *et al.* (2019) The role of Arabidopsis ABA receptors from the PYR/PYL/RCAR family in stomatal acclimation and closure signal integration. *Nat. Plants* **5**, 1002–1011.
- Dominissini, D., Moshitch-Moshkovitz, S., Schwartz, S., Salmon-Divon, M., Ungar, L., Osenberg, S., Cesarkas, K. *et al.* (2012) Topology of the human and mouse m6A RNA methylomes revealed by m⁶A-seq. *Nature* **485**, 201–206.
- Dominissini, D., Moshitch-Moshkovitz, S., Salmon-Divon, M., Amariglio, N. and Rechavi, G. (2013) Transcriptome-wide mapping of N(6)-methyladenosine by m(6)A-seq based on immunocapturing and massively parallel sequencing. *Nat. Protoc.* **8**, 176–189.
- Duan, H.C., Wei, L.H., Zhang, C., Wang, Y., Chen, L., Lu, Z., Chen, P.R. *et al.* (2017) ALKBH10B is an RNA N6-methyladenosine demethylase affecting Arabidopsis floral transition. *Plant Cell* **29**, 2995–3011.
- Fu, Y., Dominissini, D., Rechavi, G. and He, C. (2014) Gene expression regulation mediated through reversible m6A RNA methylation. *Nat. Rev. Genet.* **15**, 293–306.
- Gao, W., Long, L., Zhu, L., Xu, L., Gao, W., Sun, L., Liu, L. *et al.* (2013) Proteomic and virus-induced gene silencing (VIGS) analyses reveal that gossypol, brassinosteroids and jasmonic acid contribute to the resistance of cotton to *Verticillium dahliae*. *Mol. Cell. Proteomics* **12**, 3690–3703.
- Gupta, A., Rico-Medina, A. and Cano-Delgado, A.I. (2020) The physiology of plant responses to drought. *Science* **368**, 266–269.
- Hou, N., Li, C., He, J., Liu, Y., Yu, S., Malnoy, M., Mobeen, T.M. *et al.* (2022) MdMTA-mediated m⁶A modification enhances drought tolerance by promoting mRNA stability and translation efficiency of genes involved in lignin deposition and oxidative stress. *New Phytol.* **234**, 1294–1314.
- Hu, J., Cai, J., Park, S.J., Lee, K., Li, Y., Chen, Y., Yun, J.Y. *et al.* (2021) N6-Methyladenosine mRNA methylation is important for salt stress tolerance in Arabidopsis. *Plant J.* **106**, 1759–1775.
- Huong, T.T., Ngoc, L.N.T. and Kang, H. (2020) Functional Characterization of a putative RNA demethylase ALKBH6 in Arabidopsis growth and abiotic stress responses. *Int. J. Mol. Sci.* **21**, 6707.
- Jia, G., Fu, Y., Zhao, X., Dai, Q., Zheng, G., Yang, Y., Yi, C. *et al.* (2011) N6-methyladenosine in nuclear RNA is a major substrate of the obesity-associated FTO. *Nat. Chem. Biol.* **7**, 885–887.
- Jin, S., Zhang, X., Nie, Y., Guo, X., Liang, S. and Zhu, H. (2006) Identification of a novel elite genotype for in vitro culture and genetic transformation of cotton. *Biologia Plant* **50**, 519–524.
- Kumar, M.N., Jane, W.N. and Verslues, P.E. (2013) Role of the putative osmosensor Arabidopsis histidine kinase1 in dehydration avoidance and low-water-potential response. *Plant Physiol.* **161**, 942–953.
- Li, B., Chen, L., Sun, W., Wu, D., Wang, M., Yu, Y., Chen, G. *et al.* (2020) Phenomics-based GWAS analysis reveals the genetic architecture for drought resistance in cotton. *Plant Biotechnol. J.* **18**, 2533–2544.
- Li, L., Xing, J., Ma, H., Liu, F. and Wang, Y. (2021) In situ determination of guard cell ion flux underpins the mechanism of ABA-mediated stomatal closure in barley plants exposed to PEG-induced drought stress. *Environ. Exp. Bot.* **187**, 104468.
- Liang, C., Meng, Z., Meng, Z., Malik, W., Yan, R., Lwin, K.M., Lin, F. *et al.* (2016) GhABF2, a bZIP transcription factor, confers drought and salinity tolerance in cotton (*Gossypium hirsutum* L.). *Sci. Rep.* **6**, 35040.
- Liang, Z., Riaz, A., Chachar, S., Ding, Y., Du, H. and Gu, X. (2020) Epigenetic modifications of mRNA and DNA in plants. *Mol. Plant* **13**, 14–30.
- Liu, G., Li, X., Jin, S., Liu, X., Zhu, L., Nie, Y. and Zhang, X. (2014a) Overexpression of rice NAC gene SNAC1 improves drought and salt tolerance by enhancing root development and reducing transpiration rate in transgenic cotton. *PLoS One* **9**, e86895.
- Liu, J., Yue, Y., Han, D., Wang, X., Fu, Y., Zhang, L., Jia, G. *et al.* (2014b) A METTL3-METTL14 complex mediates mammalian nuclear RNA N6-adenosine methylation. *Nat. Chem. Biol.* **10**, 93–95.
- Liu, N., Dai, Q., Zheng, G., He, C., Parisien, M. and Pan, T. (2015) N(6)-methyladenosine-dependent RNA structural switches regulate RNA-protein interactions. *Nature* **518**, 560–564.
- Liu, Q., Wang, C., Jiao, X., Zhang, H., Song, L., Li, Y., Gao, C. *et al.* (2019) Hi-TOM: a platform for high-throughput tracking of mutations induced by CRISPR/Cas systems. *Sci. China Life Sci.* **62**, 1–7.
- Liu, G., Wang, J. and Hou, X. (2020) Transcriptome-wide N6-methyladenosine (m⁶A) methylome profiling of heat stress in Pak-choi (*Brassica rapa* ssp. *chinensis*). *Plants (Basel)* **9**, 1080.
- Lu, L., Zhang, Y., He, Q., Qi, Z., Zhang, G., Xu, W., Yi, T. *et al.* (2020) MTA, an RNA m(6)A methyltransferase, enhances drought tolerance by regulating the development of trichomes and roots in poplar. *Int. J. Mol. Sci.* **21**, 6707.
- Luo, J.H., Wang, Y., Wang, M., Zhang, L.Y., Peng, H.R., Zhou, Y.Y., Jia, G.F. *et al.* (2020) Natural variation in RNA m(6)A methylation and its relationship with translational status. *Plant Physiol.* **182**, 332–344.
- Martinez-Perez, M., Aparicio, F., Lopez-Gresa, M.P., Belles, J.M., Sanchez-Navarro, J.A. and Pallas, V. (2017) Arabidopsis m(6)A demethylase activity modulates viral infection of a plant virus and the m(6)A abundance in its genomic RNAs. *Proc. Natl. Acad. Sci. U. S. A.* **114**, 10755–10760.
- Meyer, K.D., Saletore, Y., Zumbo, P., Elemento, O., Mason, C.E. and Jaffrey, S.R. (2012) Comprehensive analysis of mRNA methylation reveals enrichment in 3' UTRs and near stop codons. *Cell* **149**, 1635–1646.
- Miao, Z., Zhang, T., Qi, Y., Song, J., Han, Z. and Ma, C. (2020) Evolution of the RNA N(6)-methyladenosine methylome mediated by genomic duplication. *Plant Physiol.* **182**, 345–360.

- Miao, Z., Zhang, T., Xie, B., Qi, Y. and Ma, C. (2022) Evolutionary implications of the RNA N6-methyladenosine methylome in plants. *Mol. Biol. Evol.* **39**, msab299.
- Pendleton, K.E., Chen, B., Liu, K., Hunter, O.V., Xie, Y., Tu, B.P. and Conrad, N.K. (2017) The U6 snRNA m(6A) methyltransferase METTL16 regulates SAM synthetase Intron retention. *Cell* **169**, 824–835.
- Ping, X.L., Sun, B.F., Wang, L., Xiao, W., Yang, X., Wang, W.J., Adhikari, S. et al. (2014) Mammalian WTAP is a regulatory subunit of the RNA N6-methyladenosine methyltransferase. *Cell Res.* **24**, 177–189.
- Ren, Z., Tang, B., Xing, J., Liu, C., Cai, X., Hendy, A., Kamran, M. et al. (2022) MTA1-mediated RNA m⁶A modification regulates autophagy and is required for infection of the rice blast fungus. *New Phytol.* **235**, 247–262.
- Rodrigues, J., Inze, D., Nelissen, H. and Saibo, N.J.M. (2019) Source-sink regulation in crops under water deficit. *Trends Plant Sci.* **24**, 652–663.
- Růžicka, K., Zhang, M., Campilho, A., Bodi, Z., Kashif, M., Saleh, M., Eeckhout, D. et al. (2017) Identification of factors required for m6A mRNA methylation in Arabidopsis reveals a role for the conserved E3 ubiquitin ligase HAKAI. *New Phytol.* **215**, 157–172.
- Saxena, I., Srikanth, S. and Chen, Z. (2016) Cross Talk between H₂O₂ and interacting signal molecules under plant stress response. *Front. Plant Sci.* **7**, 570.
- Schmittgen, T.D. and Livak, K.J. (2008) Analyzing real-time PCR data by the comparative C_T method. *Nat. Protoc.* **3**, 1101–1108.
- Scutenaire, J., Deragon, J.M., Jean, V., Benhamed, M., Raynaud, C., Favory, J.J., Merret, R. et al. (2018) The YTH domain protein ECT2 is an m(6A) reader required for normal trichome branching in Arabidopsis. *Plant Cell* **30**, 986–1005.
- Shang, X., Yu, Y., Zhu, L., Liu, H., Chai, Q. and Guo, W. (2020) A cotton NAC transcription factor GhIRNAC2 plays positive roles in drought tolerance via regulating ABA biosynthesis. *Plant Sci.* **296**, 110498.
- Song, P., Yang, J., Wang, C., Lu, Q., Shi, L., Tayier, S. and Jia, G. (2021) Arabidopsis N(6)-methyladenosine reader CPSF30-L recognizes FUE signals to control polyadenylation site choice in liquid-like nuclear bodies. *Mol. Plant* **14**, 571–587.
- Su, Z., Ma, X., Guo, H., Sukiran, N.L., Guo, B., Assmann, S.M. and Ma, H. (2013) Flower development under drought stress: morphological and transcriptomic analyses reveal acute responses and long-term acclimation in Arabidopsis. *Plant Cell* **25**, 3785–3807.
- Su, T., Fu, L., Kuang, L., Chen, D., Zhang, G., Shen, Q. and Wu, D. (2022) Transcriptome-wide m⁶A methylation profile reveals regulatory networks in roots of barley under cadmium stress. *J. Hazard. Mater.* **5**, 423.
- Sun, J., Bie, X., Wang, N., Zhang, X. and Gao, X. (2020) Genome-wide identification and expression analysis of YTH domain-containing RNA-binding protein family in common wheat. *BMC Plant Biol.* **20**, 351.
- Tardieu, F., Simonneau, T. and Muller, B. (2018) The physiological basis of drought tolerance in crop plants: A scenario-dependent probabilistic approach. *Annu. Rev. Plant Biol.* **69**, 733–759.
- Wang, Y., Li, Y., Toth, J.I., Petroski, M.D., Zhang, Z. and Zhao, J.C. (2014) N6-methyladenosine modification destabilizes developmental regulators in embryonic stem cells. *Nat. Cell Biol.* **16**, 191–198.
- Wang, X., Zhao, B.S., Roundtree, I.A., Lu, Z., Han, D., Ma, H., Weng, X. et al. (2015) N(6)-methyladenosine modulates messenger RNA translation efficiency. *Cell* **161**, 1388–1399.
- Wang, X., Wang, H., Liu, S., Ferjani, A., Li, J., Yan, J., Yang, X. et al. (2016a) Genetic variation in ZmVPP1 contributes to drought tolerance in maize seedlings. *Nat. Genet.* **48**, 1233–1241.
- Wang, X., Feng, J., Xue, Y., Guan, Z., Zhang, D., Liu, Z., Gong, Z. et al. (2016b) Structural basis of N6-adenosine methylation by the METTL3–METTL14 complex. *Nature* **534**, 575–578.
- Wang, P., Zhang, J., Sun, L., Ma, Y., Xu, J., Liang, S., Deng, J. et al. (2018) High efficient multisites genome editing in allotetraploid cotton (*Gossypium hirsutum*) using CRISPR/Cas9 system. *Plant Biotechnol. J.* **16**, 137–150.
- Wang, M., Tu, L., Yuan, D., Zhu, D., Shen, C., Li, J., Liu, F. et al. (2019) Reference genome sequences of two cultivated allotetraploid cottons, *Gossypium hirsutum* and *Gossypium barbadense*. *Nat. Genet.* **51**, 224–229.
- Wang, W., Li, W., Cheng, Z., Sun, J., Gao, J., Li, J., Niu, X. et al. (2022) Transcriptome-wide N6-methyladenosine profiling of cotton root provides insights for salt stress tolerance. *Environ. Exp. Bot.* **194**, 104729.
- Wei, W., Ji, X., Guo, X. and Ji, S. (2017) Regulatory role of N6-methyladenosine (m⁶A) methylation in RNA processing and human diseases. *J. Cell. Biochem.* **118**, 2534–2543.
- Wei, L.H., Song, P., Wang, Y., Lu, Z., Tang, Q., Yu, Q., Xiao, Y. et al. (2018) The m(6A) Reader ECT2 controls trichome morphology by affecting mRNA stability in Arabidopsis. *Plant Cell* **30**, 968–985.
- Xu, C., Wang, X., Liu, K., Roundtree, I.A., Tempel, W., Li, Y., Lu, Z. et al. (2014) Structural basis for selective binding of m6A RNA by the YTHDC1 YTH domain. *Nat. Chem. Biol.* **10**, 927–929.
- Yang, D., Xu, H., Liu, Y., Li, M., Ali, M., Xu, X. and Lu, G. (2021) RNA N6-methyladenosine responds to low-temperature stress in tomato anthers. *Front. Plant Sci.* **12**, 687826.
- Yue, Y., Liu, J., Cui, X., Cao, J., Luo, G., Zhang, Z., Cheng, T. et al. (2018) VIRMA mediates preferential m6A mRNA methylation in 3' UTR and near stop codon and associates with alternative polyadenylation. *Cell Discov.* **4**, 10.
- Zhang, F., Zhang, Y.C., Liao, J.Y., Yu, Y., Zhou, Y.F., Feng, Y.Z., Yang, Y.W. et al. (2019) The subunit of RNA N6-methyladenosine methyltransferase OsFIP regulates early degeneration of microspores in rice. *PLoS Genet.* **15**, e1008120.
- Zhang, G., Lv, Z., Diao, S., Liu, H., Duan, A., He, C. and Zhang, J. (2021) Unique features of the m⁶A methylome and its response to drought stress in sea buckthorn (*Hippophae rhamnoides* Linn.). *RNA Biol.* **18**, 794–803.
- Zhao, X., Yang, Y., Sun, B.F., Shi, Y., Yang, X., Xiao, W., Hao, Y.J. et al. (2014) FTO-dependent demethylation of N6-methyladenosine regulates mRNA splicing and is required for adipogenesis. *Cell Res.* **24**, 1403–1419.
- Zhao, B.S., Roundtree, I.A. and He, C. (2017) Post-transcriptional gene regulation by mRNA modifications. *Nat. Rev. Mol. Cell Biol.* **18**, 31–42.
- Zheng, G., Dahl, J.A., Niu, Y., Fedorcsak, P., Huang, C.M., Li, C.J., Vagbo, C.B. et al. (2013) ALKBH5 is a mammalian RNA demethylase that impacts RNA metabolism and mouse fertility. *Mol. Cell* **49**, 18–29.
- Zheng, H., Sun, X., Li, J., Song, Y., Song, J., Wang, F., Liu, L. et al. (2021) Analysis of N6-methyladenosine reveals a new important mechanism regulating the salt tolerance of sweet sorghum. *Plant Sci.* **304**, 110801.
- Zhong, S., Li, H., Bodi, Z., Button, J., Vespa, L., Herzog, M. and Fray, R.G. (2008) MTA is an Arabidopsis messenger RNA adenosine methylase and interacts with a homolog of a sex-specific splicing factor. *Plant Cell* **20**, 1278–1288.
- Zhou, J., Wan, J., Gao, X., Zhang, X., Jaffrey, S.R. and Qian, S.B. (2015) Dynamic m(6A) mRNA methylation directs translational control of heat shock response. *Nature* **526**, 591–594.
- Zhou, C., Wang, C., Liu, H., Zhou, Q., Liu, Q., Guo, Y., Peng, T. et al. (2018) Identification and analysis of adenine N(6)-methylation sites in the rice genome. *Nat. Plants* **4**, 554–563.
- Zhou, L., Tian, S. and Qin, G. (2019) RNA methylomes reveal the m(6A)-mediated regulation of DNA demethylase gene *SIDML2* in tomato fruit ripening. *Genome Biol.* **20**, 156.
- Zhou, L., Tang, R., Li, X., Tian, S., Li, B. and Qin, G. (2021) N6-methyladenosine RNA modification regulates strawberry fruit ripening in an ABA-dependent manner. *Genome Biol.* **22**, 168.
- Zhou, L., Gao, G., Tang, R., Wang, W., Wang, Y., Tian, S. and Qin, G. (2022) m⁶A-mediated regulation of crop development and stress responses. *Plant Biotechnol. J.* **2022**, 1447–1455.

Supporting information

Additional supporting information may be found online in the Supporting Information section at the end of the article.

Figure S1. Correlation analyses of two biological replicates of MeRIP-seq and mRNA-seq under different drought conditions of variety ZY7.

Figure S2. Correlation analyses of two biological replicates of MeRIP-seq and mRNA-seq under different drought conditions of variety ZY168.

Figure S3. Saturation analyses of the MeRIP peak count in each sample under different drought conditions.

Figure S4. Number of consistent peaks and transcripts under different conditions.

Figure S5. Correlation analyses between the fold change of m⁶A enrichment and mRNA abundance of significant DMeTs under drought conditions.

Figure S6. The cumulative curve for peaks enriched in different region in ZY7 and ZY168.

Figure S7. Venn plot for the shared significant DMeTs under different conditions in the same variety of ZY7 and ZY168, respectively.

Figure S8. GO analyses for DMeTs in ZY168 under different drought conditions.

Figure S9. KEGG analyses for DMeTs in ZY7 and ZY168 under different drought conditions.

Figure S10. Phylogenetic tree for *ALKBH* genes in *Arabidopsis* and *Gossypium hirsutum*.

Figure S11. FPKM of *GhALKBH9* and *GhALKBH10* under different drought conditions in ZY7 and ZY168.

Figure S12. Generation of mutants for *GhALKBH9A* and *GhALKBH9B* demethylase genes in cotton.

Figure S13. Characterizations of m⁶A demethylase gene *GhALKBH10A* in cotton response to drought stress.

Figure S14. Frame of amino acid sequence of wild type and mutants of *alkbh10b*.

Figure S15. Characterizations of m⁶A demethylase genes *GhALKBH9A* and *GhALKBH9B* in cotton response to drought stress.

Figure S16. Negative control genes involved in ABA and Ca²⁺ response.

Figure S17. m⁶A-IP-qPCR assay showing the relative m⁶A enrichment in wild type and mutant plants for *Ghalkbh9a* and *Ghalkbh9b*.

Figure S18. The dynamic expression level of *GhECA1* and *GhCNGC4* in drought resistant and drought sensitive varieties under different drought conditions.

Figure S19. Phenotypes of *Ghmta* and *Ghfp37* plants in the field.

Figure S20. Gel of fragment mRNA in m⁶A-IP-qPCR assay.

Figure S21. Detecting net Ca²⁺ flux of cotton mesophyll cells by Non-invasive Micro-test Technology (NMT).

Table S1. MeRIP-seq and mRNA-seq information of two cotton varieties.

Table S2. Number of m⁶A peak and transcript detected under different drought conditions.

Table S3. DMeTs contained CAAUG sequence in and near 5'UTR.

Table S4. Information of differentially m⁶A-enriched peaks within significant DMeTs identified in ZY7.

Table S5. Information of differentially m⁶A-enriched peaks within significant DMeTs identified in ZY168.

Table S6. GO analyses for DMeTs in ZY7 under MD.

Table S7. GO analyses for DMeTs in ZY7 under SD.

Table S8. GO analyses for DMeTs in ZY7 under RD.

Table S9. GO analyses for DMeTs in ZY168 under MD.

Table S10. GO analyses for DMeTs in ZY168 under SD.

Table S11. KEGG analyses for DMeTs in ZY7 under different drought conditions.

Table S12. KEGG analyses for DMeTs in ZY168 under different drought conditions.

Table S13. Information of homologous demethylase genes in *Gossypium hirsutum*.

Table S14. List of all genes with DMeTs in cotton.

Table S15. Information of homologous methyltransferase genes in this study.

Table S16. List of primers used in this study.

Data S1. MeRIP-seq, mRNA-seq and data analysis.